Quantifying the global solar radiation received in Pietermaritzburg, KwaZulu-Natal using a temperature based method (Hargreaves-Samani) to determine the Angstrom coefficients through the clearness index.

by

TAMARA ROSEMARY GOVINDASAMY

Submitted in partial fulfilment of the academic requirements of

Master of Science in Physics

School of Chemistry and Physics
College of Agriculture, Engineering and Science
University of KwaZulu-Natal
Pietermaritzburg

2015

Contents Page

Declaration

This dissertation describes the work undertaken in the School of Chemistry and Physics, University of KwaZulu-Natal (Pietermaritzburg), under the supervision of Dr. N. Chetty, between January 2014 - November 2015. I declare this to be my original work except where due reference and credit is given.

Student : Tamara Rosemary Govindasamy

Signature: .....

Date: .....

Supervisor: Dr. Naven Chetty

Signature: .....

Date: .....

Acknowledgments

- Firstly, all praise and thanks to God for the strength and courage to pursue my dreams. My faith in Him has brought me this far.

- I am truly grateful to my supervisor, Dr. N. Chetty for all his hard work and support. He has encouraged and assisted me throughout the past few years. Thank you for your patience and motivation.

- This work is dedicated to my late parents, Mr. and Mrs. Govindasamy. Your perseverance and life lessons have laid the foundation of the path I intend to follow.

- A special thank you to Mr. R. Sivraman and Mr. K. Penzhorn for their assistance at any given hour. You guys are the backbone of our department.

- I would like to acknowledge the financial support received from the NRF-DAAD for the commencement of this research.

- A huge thank you to Mr. Richard Kunz of the University of KwaZulu-Natal Research Center in Ukulinga (Bisley); the ARC (Cedara) for providing the required data from the Ukulinga Research Farm.

- Lastly I would like to express my sincere gratitude to my family and friends for all their encouragement and support. Athene and Marlen Govindasamy, who have moulded me and always kept me focused. I am blessed to have you all in my life.

List of Figures and Tables

Page

Abstract

South Africa's power utility, ESKOM, is currently in a state of crisis due to the aging infrastructure, old technology and the rapid depletion of coal resources and other fossil fuels. Load shedding (regularly scheduled power outages) has impacted on the country's economy as well as the lives of all citizens. Application of renewable energy sources are constantly sought after as the cost of grid electricity continues to peak. Solar radiation is an environmentally friendly and inexhaustible energy resource which has the potential to supply global energy demands. In this study, we propose a method for estimating the Global Solar Radiation (GSR) incident in Pietermaritzburg, the capital city of KwaZulu-Natal, South Africa, to promote the use of this unlimited energy resource. Records of solar radiation for this city are limited by the high costs associated with the required instrumentation for measuring incident solar radiation. Most local weather stations find it too expensive to measure this meteorological parameter in every city.

Our work involved daily measurements of maximum and minimum air temperatures for three suburbs in Pietermaritzburg namely; Northdale, Scottsville and Bisley for a period of one calendar year (July 2014 - June 2015). The Hargreaves Samani model was used to predict the daily amounts of GSR (H) and Extraterrestrial Radiation (ETR) (H_o) for each town. These computed values were then compared to data measured by the Agricultural Research Council (ARC). Results indicated an overall strong agreement between the measured values and predicted values of this work. An annual average RMSE (Root Mean Square Error) between the measured and calculated values was found to be no greater than 4.40. Following the Angstrom-Prescott approach, H and H_o values were modeled against the relative sunshine duration data to determine the Angstrom coefficients. In this work, we have obtained a model to determine GSR in each of the suburbs, by utilizing the computed Angstrom coefficients. This thus serves as a second simple method to predict the GSR incident in

Pietermaritzburg. Using a linear fit for these variables yielded the annual average Angstrom coefficients to be; $a = 0.24 \pm 0.07$ and $b = 0.40 \pm 0.06$. These coefficients need to be further observed by monitoring the solar radiation data for Pietermaritzburg over a longer study period. Prediction of solar radiation for a location is crucial in the design and development of solar Photovoltaic (PV) technologies. This data can also be used to determine the optimal spot for placement of these technologies. The models discussed in this study prove to be reliable and sufficient in the estimation of solar radiation in Pietermaritzburg, and can be employed by weather stations where measurements are not conducted.

Chapter 1

Introduction

1.1. Introduction

Solar energy is a pure, inexhaustible, and readily available resource. The increase in price of conventional energy sources, together with the depletion of non-renewable resources and fossil fuels, necessitates a great demand for alternative power sources. Green energy sources which are beneficial to the environment, are being studied as alternate resources which could potentially aid in the energy crisis. The cost of these technologies has reduced significantly in the past decade, however it still remains higher than the cost of conventional energy and hence uptake is still relatively slow [1].

With the current state of energy in South Africa, load shedding has become a part of every citizens daily regime. When resources run low power outages are implemented. There is a great cause for concern with the depletion of the coal resources and the constant strain which is placed on existing resources and power stations [2]. The state's power utility, ESKOM, is unable to cope with the current demand of electricity production and supply which has led to the introduction of the load shedding policy [3,4,5]. With the growing shortage of energy supply and now load shedding, the South African economy is facing dire consequences as industries are unable to function at their maximum capacity [6]. Energy generation infrastructure is under constant strain in order to meet the country's demands, which has consequently resulted in a huge increase in production costs. Thus leaving citizens with a heavier bill to fit, while still having the experience of both planned and unplanned power outages [3,4,5,7].

The economy in South Africa is considered to be 'energy-intensive' with its primary de-

pendence being on the energy supplied from coal resources [7]. The energy demand has significantly increased with the expansion of industry and residential energy consumption [6,7]. South Africa's energy intensity is relatively high in comparison to other developing countries [7]. The conservation of energy resources, together with the sustainable use of energy has become the prime focus to ensure energy security for the country's future [3,7]. Government has implemented energy policies to meet the security crises, but these fail without proper implementation [3].

Policies which promote the efficient use of energy and the utilization of new renewable technologies are restricted by their accessibility and affordability within the residential sector [3,7]. Whilst most high-income households are more accepting to the use of newer technologies for greener energy supply, the poorer consumers are unable to afford basic tariffs for energy supply [7]. Both the industrial and residential sectors have initiated the effective use of energy through various energy saving techniques [7]. These include the employment of efficient lighting systems (Compact Fluorescent Lighting), heating and cooling systems, Solar Water Heaters, geyser blankets, the use of alternate fuels such as Liquified Petroleum gases and thermal savers [7]. Though the costs of new energy technologies has reduced due to their large scale production and promotion, they remain unavailable to the common consumer [7]. These are some of the concerns which government has set out to address so that the access to these energy efficient interventions are actually put into practice. There is a dire need for more significant interventions to be made to address these concerns [3,4].

Almost 95% of the electricity demand in South Africa is met by the energy produced from coal [3]. This resource is rapidly diminishing, hence alternate renewable energy resources such as nuclear, wind, hydro and solar are being considered [2,3,6,7]. Nuclear power currently contributes a small fraction to the energy supplied by power stations in our country, while the other resources have not fully found their place [3,7]. The climate in South Africa makes it ideal for the initialization of hydro-electric and solar powered stations [8]. The

utilization of these renewable technologies will also reduce South Africa's carbon footprint. Being an economy which has a high dependence on coal resources, our country has a high rate of Green House Gas (GHG) emissions [5,7]. On a global scale, this contribution will aid in the rescue of our planet from global warming and its intense consequences.

Significant growth in solar energy technologies has been noted, together with its theoretical potential to supply the global demand for energy being the major contributing factor [1]. South Africa is well suited for the harnessing of solar radiation because sunshine is available throughout the year including the winter months. Depending on the geographical location certain areas in Africa receive more than double the amount of radiation as compared to countries in the northern hemisphere [6]. Despite this abundance, there are many financial and technical restraints with regards to solar energy technologies, which limits its use to private off-grid connections. These limitations need to be overcome in order to increase the contribution of solar power to the energy supply of the country.

The amount of solar radiation received at the surface of the earth is a measurable quantity [9]. Solar radiation incident outside of the earth's atmosphere, received at a surface which is normal to the incident radiation is known as the solar constant [9,10]. This quantity is measured from space through the use of satellite data and has a value of 1367 Wm^{-2}, which changes by approximately 0.01% over a period of 30 years [10-14]. The amount of solar radiation received at the earth's surface is depleted by about 50% as compared to its original value as depicted in Figure 1: An illustration of the Earth-Sun Energy Budget [11,12] . This is due to the attenuation processes which occur in the atmosphere, with almost 30% of the incident radiation being reflected before reaching the Earth's surface [11,12].

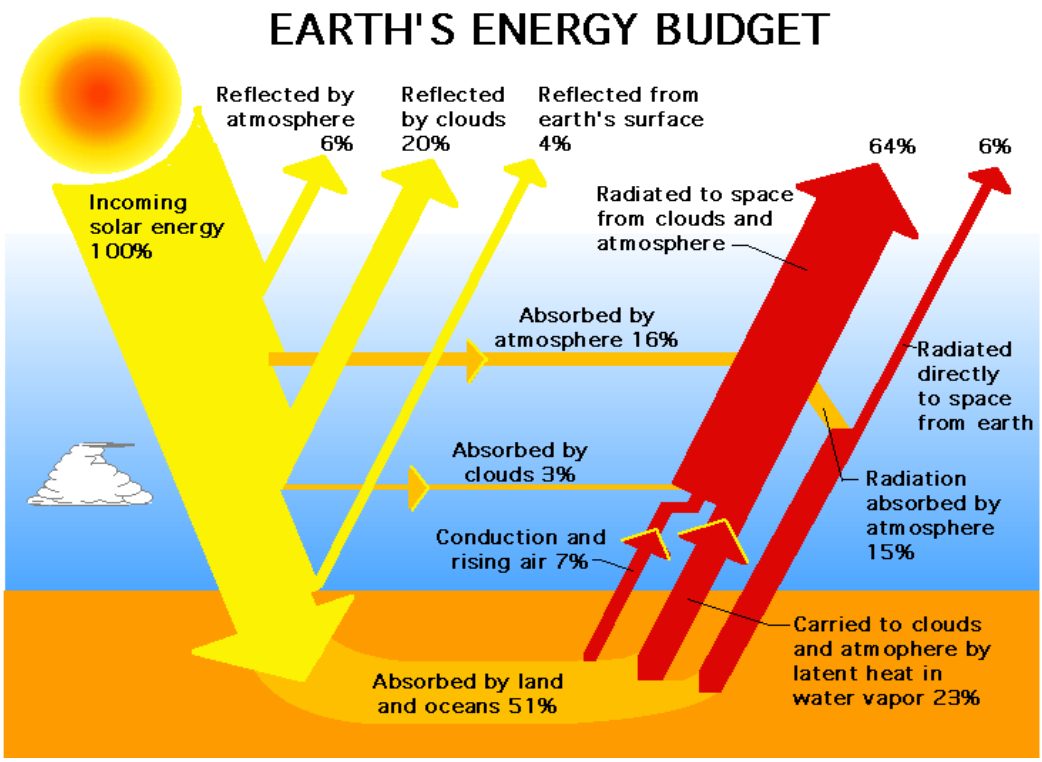

Figure 1: An illustration of the Earth-Sun energy budget [12].

Global Solar Radiation (GSR) is the total solar radiation irradiating a horizontal surface and it comprises of two components; Diffuse Solar Radiation and Direct Solar Radiation [9-13]. When the radiation passes through the atmosphere, it undergoes the effects of reflection, absorption and scattering. The irradiance which is scattered from all directions is known as Diffuse Solar Radiation [11,13]. While some of the incident radiation will also be back scattered and reflected into space by the Earth's surface, the radiation that enters the Earth's surface in a straight line is called Direct Solar Radiation [9-11,13-15].

Solar radiation is responsible for many processes which occur on the earth's surface and its research finds applications in many science and engineering fields [16]. Knowledge and prediction of solar radiation available at a specific location is of great importance for the designing and performance evaluation of solar energy conversion systems [16,17]. Solar energy can be harnessed and utilized for applications which fall into two main categories; Solar

Thermal and Solar Photovoltaic (PV) [1, 16,17].

In many geographical locations, Global Solar Radiation (GSR) is not measured because it is too expensive to purchase and maintain the apparatus required. If measured data is available it is not always complete as equipment can fail due to numerous faults [16,18]. As a result, accurate and efficient forecasting methods are increasingly required. Hence researchers have employed the use of empirical methods which are able to calculate and predict GSR for a particular location [10,16,18-20].

Many of these empirical models require the input of other meteorological variables (which are often more readily available than solar radiation data) or historical weather data. Some of these meteorological parameters include; air temperature, precipitation, relative humidity, sunshine duration, etc. [18-20]. The empirical model is classified according to the climatic variable which it requires [16], e.g. sunshine duration models [17,20-23], temperature based methods [16,24-26], and cloud-based methods which require the use of satellite sky images [11].

In this work, we have quantified the GSR received in three suburbs in Pietermaritzburg by using readily available meteorological data (maximum and minimum temperatures, sunshine duration). The study was conducted over one calendar year (July 2014 - June 2015). The Angstrom coefficients for this study period were obtained through relevant calculations. A reliable set of these empirical coefficients will allow for a second simple method for the forecasting of GSR in Pietermaritzburg as well as geographical locations with similar climatic conditions. The current state of energy in our country has given a reason to investigate the use of solar powered technologies, which are now available on the market. Prediction of the amount of GSR incident across this city, enables for optimal placement of these solar PV technologies. Introduction of these alternate energy sources within the industrial and residential sectors could possibly alleviate the strain placed on the city's grid-connection.

Chapter 2

Background and Theory

2.1. Climate in South Africa, KwaZulu-Natal

The South African climate is strongly influenced by its geographical position in the Southern Hemisphere with respect to the equator, its regional topography and the effects of the surrounding Atlantic and Indian oceans [8]. The climatic conditions experienced here are described as semi-arid with inconsistently high rainfall and a high occurrence of weather extremes [8,27]. The country's landscape extends itself over a range of altitudes, with the highest being in the Drakensberg Mountain Range (3000 m +) [8,28]. The coastal regions of South Africa experience a sub-tropical climate (hot and humid weather conditions), while the southern parts of South Africa have a mediterranean climate (hot, dry summers and warm, wet winters) [8,27,28].

This climate directly affects the country's population, biological processes and hence the economy. The rainfall, temperatures and relative humidity experienced throughout the year are direct indicators of season change [8,27,28]. Summer extends over the December to February months, Autumn in March to May, Winter in June to August, and Spring is experienced in September through until November. South Africa receives most of its rainfall during the summer months (high cloud cover), but is still able to maintain a constant clearness index over all seasons [8,27]. The clearness index is a indicator of the atmosphere's degree of transparency [11]. Overall, South Africa's warm climate is mostly due to the amount of sunshine received [6].

South Africa receives high quantities of solar radiation throughout the year and on aver-

age this lies in the range of; $16.2\,MJ/m^2\,to\,23.4\,MJ/m^2$ per day [6,29]. This value is higher than those received in countries of the Northern Hemisphere [6]. The North Eastern provinces in South Africa are where the largest amounts of Direct Normal solar radiation are experienced. These provinces which include the Free State, Northern Cape and Eastern Cape are capable of running Concentrating Solar Power (CSP) plants, as they have an average GSR value exceeding $25.2\,MJ/m^2$ [1,29]. CSP plants constitute arrays of solar panels to capture solar radiation at a large-scale for possible grid utility supply [29].

Pietermaritzburg is the capital city of KwaZulu-Natal, an eastern, coastal province in South Africa. It is also known as the Midlands Region. The climate of this province is sub-tropical and influenced by the atmospheric circulation which is affected by the Indian Ocean and the escarpment (Drakensberg Mountains) [8,28]. The province experiences the highest rainfall in South Africa but is still one of the warmest [28]. Pietermaritzburg, being located closer to the mountains experiences more temperature variation due to the atmospheric pressure, rather than the effects of humidity from the coastline [8,28]. This city is situated approximately 80 km away from the coast and is surrounded by the escarpment, hence the city is in a basin or hollow [28]. Due to its location with regards to the coastline, Pietermaritzburg is seen as an inland city. Annual average minimum temperatures for Pietermaritzburg, range from $16^oC\,to\,18^oC$ as depicted in Figure 2 [28]. GSR received in this city may not be suitable for large scale solar power plants, however this study shows that it receives ample solar radiation for the application of passive solar PV technologies.

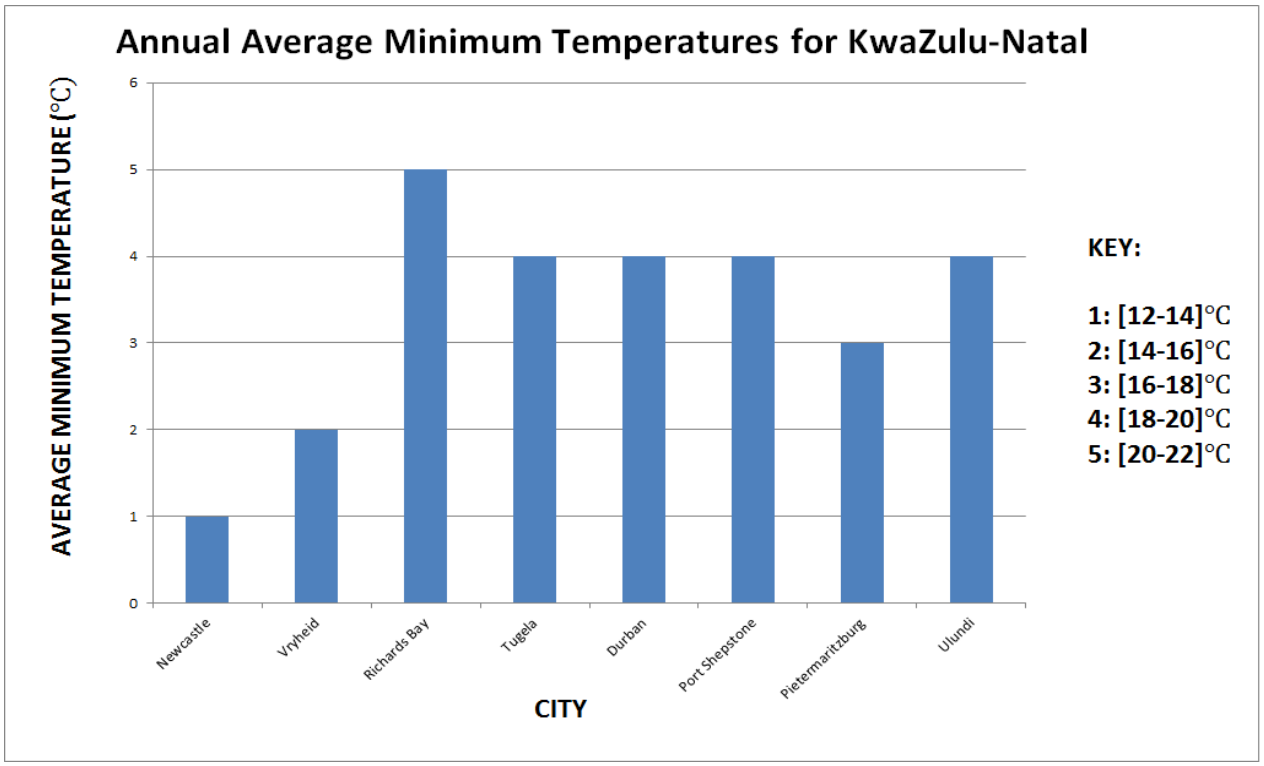

Figure 2: Annual Average minimum temperatures for KwaZulu-Natal [28].

2.2. Solar Radiation

The electromagnetic radiation emitted from the Sun (Solar Radiation), is the main source of energy for life to exist on Earth. This radiation is responsible for many of the physical and biological processes which occur on Earth and is also the main source of the climate we experience [9,11]. The rays of radiation from the Sun are almost nearly parallel and have to pass through the Earth's atmosphere. The Extraterrestrial radiation (ETR) (H_o) which is incident on a surface outside the Earth's atmosphere and normal to the incident radiation from the Sun is known as the Solar Constant, $I_{sc} = 1367\, W/m^2$ (At mean Sun-Earth distance) [9,11,30,31]. Studies conducted by the World Radiation Center (WRC) and the National Aeronautics and Space Administration (NASA), show that this Solar Constant is not expected to show much variation in the years to come, despite its discrepancies in spectral

distribution [11,30,31]. The Solar Constant is studied to better understand the proportion of radiation entering the atmosphere and subsequently the climate expected on Earth [9].

2.2.1. Components of Solar Radiation

Upon entering the Earth's atmosphere, the parallel light rays undergo attenuation through processes like scattering, reflection and only a portion of the incident radiation is absorbed by the Earth's surface [9-11,30-32]. Scattering of the radiation mainly occurs at short wavelengths and is due to the particles which constitute the atmosphere [10,11]. Water vapor (clouds), aerosols and other particles which are found in the Earth's atmosphere, cause the incident radiation to be scattered into random directions [9,11,32]. This is known as Diffuse Radiation (H_D) [11,30-32]. These gases and particles can also absorb the radiation as illustrated in Figure 3. Reflection occurs at the surface of the Earth and at an atmospheric level, where a portion of the incident radiation is reflected back into space. Surface Albedo is defined as the ratio of the reflected solar radiation to the incoming solar radiation (explained in section 2.2.4.1.) [32]. The remaining radiation which irradiates a horizontal surface on the Earth is called Direct Beam Radiation (H_B) [9,11,30-32].

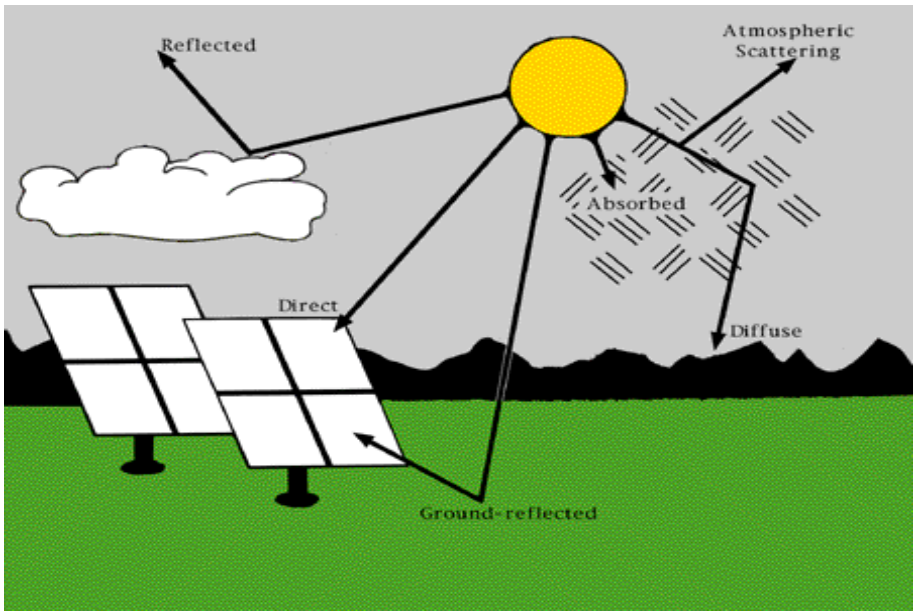

Figure 3: Attenuation of incoming solar radiation [11]

Global Solar Radiation (GSR), denoted by H (MJ/m^2), is the total radiation received on a horizontal surface, i.e. the sum of the Diffuse and Direct Beam radiation components [11,31,33];

$$H = H_D + H_B. \tag{1}$$

The term 'global' is used as it represents the radiation received from all angles [31]. While the total solar radiation irradiating a non-horizontal surface on Earth H_T has to include the ground reflected radiation H_R [9,11,31];

$$H_T = H_D + H_B + H_R, \tag{2}$$

Lambert's Cosine Law is used to describe the GSR incident on a horizontal surface with respect to its angle of incidence with the surface. The angle at which the nearly parallel radiation beams are incident to the horizontal surface is equal to the solar zenith angle (θ_z) [11,30,31]. Hence, for a horizontal surface the total GSR can be described by;

$$H = H_D + H_o \, cos\theta_z. \tag{3}$$

and for a non-horizontal surface, the total incident radiation is

$$H_T = H_D + H_o\, cos\theta_i\ + H_R, \tag{4}$$

where θ_i is the angle of incidence between the beam and is measured with respect to the normal of the tilted surface [31].

The ratio of the GSR (H) to the ETR (H_o) gives a description of the atmosphere's transparency and is called the Clearness Index (K_T) [11].

$$K_T = \frac{H}{H_o}. \tag{5}$$

This will be further discussed in Section 2.4.

2.2.2. Solar Geometry (Sun Angles)

To determine the actual amount of solar radiation received on Earth, the Sun's position has to be considered. The position of the Sun varies throughout the day and thus to locate the Sun (with respect to Earth), it is important to consider the Sun's zenith angle (θ_z), altitude (α), and the azimuth angle (γ) [10,33,34]. The Earth's orbit around the Sun is elliptical and has an axial tilt of 23.45^o as described in [34-37]. As it orbits the Sun, the Earth's axis of rotation remains in a fixed position and this leads to seasonal variation [36,37].The celestial equator is the projection of the Earth's equatorial plane, which is used to understand it's position.

When the celestial equator intersects with the ecliptic plane, the Earth experiences Equinoxes [36,37]. Equinoxes are indicators of season change. The Sun passes the Earth's equator, whilst it is south bound and this is known as the Vernal Equinox in the Southern Hemisphere [10,36,37]. This occurs on the 23rd of September each year, with the Autumnal

Equinox on the 21st of March [10,36,37]. When the Earth is closest or furthest away from the Sun, Solstices are experienced. This occurs twice a year. June 21st is known as the Winter Solstice in the Southern Hemisphere and this is when the shortest day and longest night occur, due to the lowest sun angle of the year [36,37]. On December 21st the Summer Solstice brings the longest day corresponding to the largest sun angle for the year [10,36,37].

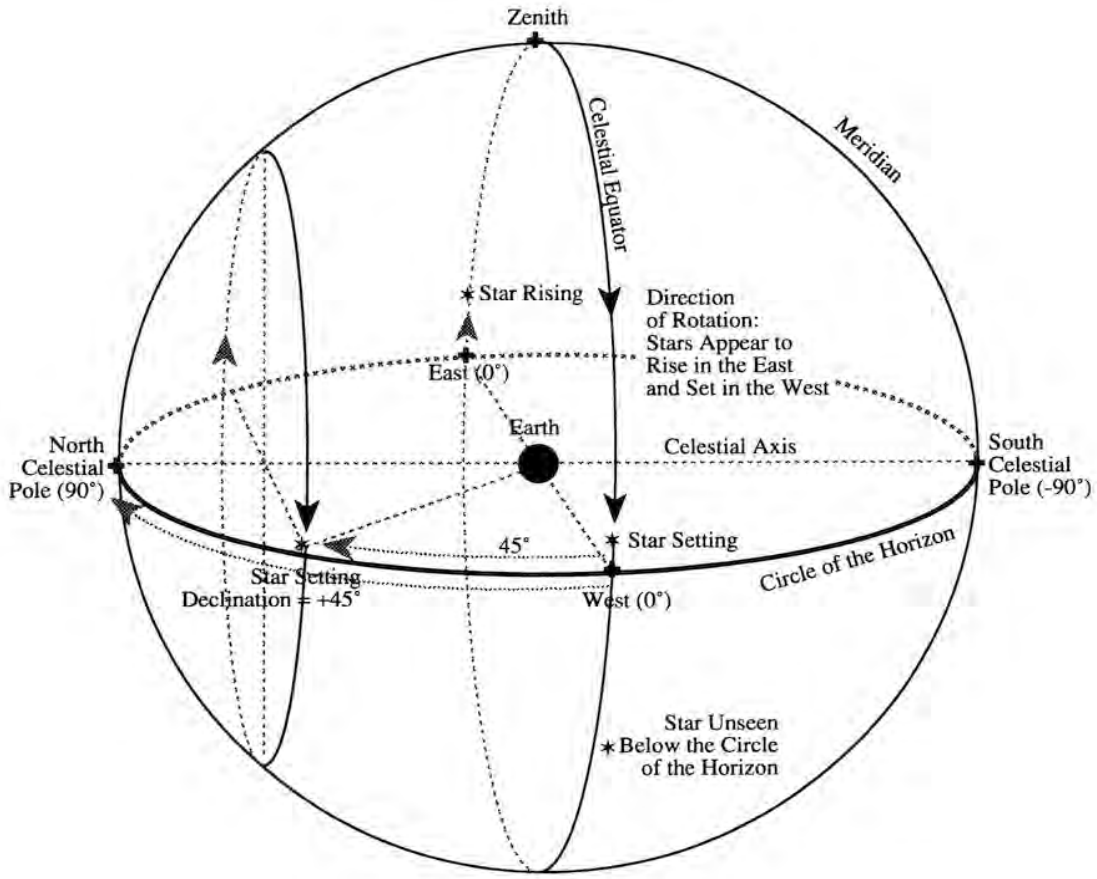

Figure 4: The intersections of the celestial sphere [38]

The solar radiation incident on a surface on the Earth is also dependent on the latitude of that particular location. A specific site will receive the highest amount of solar radiation when the sun reaches it's zenith which is it's highest point in the sky for that particular day [35-37]. The specific time when the Sun is at its peak, is known as the Solar Noon. The zenith angle is dependent on the latitude of the location (ϕ), the time of day (t), solar noon

(t_o) and the solar declination (δ) [33].

$$cos\theta_z = sin\phi sin\delta + cos\phi cos\delta cos[15(t - t_o)]. \tag{6}$$

The time of solar noon and time of day need to be converted from hours to degrees, so it is multiplied by a factor of 15 ($\frac{360^o}{24\,hours} = 15$) [11,33].

The latitude of a site (ϕ) is negative if it is in the Southern Hemisphere, positive for the Northern Hemisphere and its value ranges from $0^o - 90^o$ [10,11,33]. This quantity is available for all geographical locations in any standard atlas.

The declination angle (δ), is defined as the angle at which the Sun is located directly above the site, or at its zenith [11,33] and is given by the expression in [11,17,23,33] as;

$$\delta = 23.45^o sin\left[360^o \frac{(284 + D_n)}{365}\right], \tag{7}$$

δ is a function of the Julian calendar day D_n(Jan 1st = 1, Dec 31st = 365) [17,23,33], as well as the obliquity of the Earth's orbit.

The hour angle (ω_s) is the time deviation (in degrees) from solar noon [11,23,37];

$$\omega_s = cos^{-1}(-tan\phi tan\delta). \tag{8}$$

The solar azimuth angle (γ) is the angle measured from the North or South of the Earth in the horizontal plane [33]. This angle is measured with respect to the south and increases, counter-clockwise [11,33];

$$cos\gamma = -\frac{(sin\delta - cos\theta_z sin\phi)}{cos\phi sin\theta_z}. \tag{9}$$

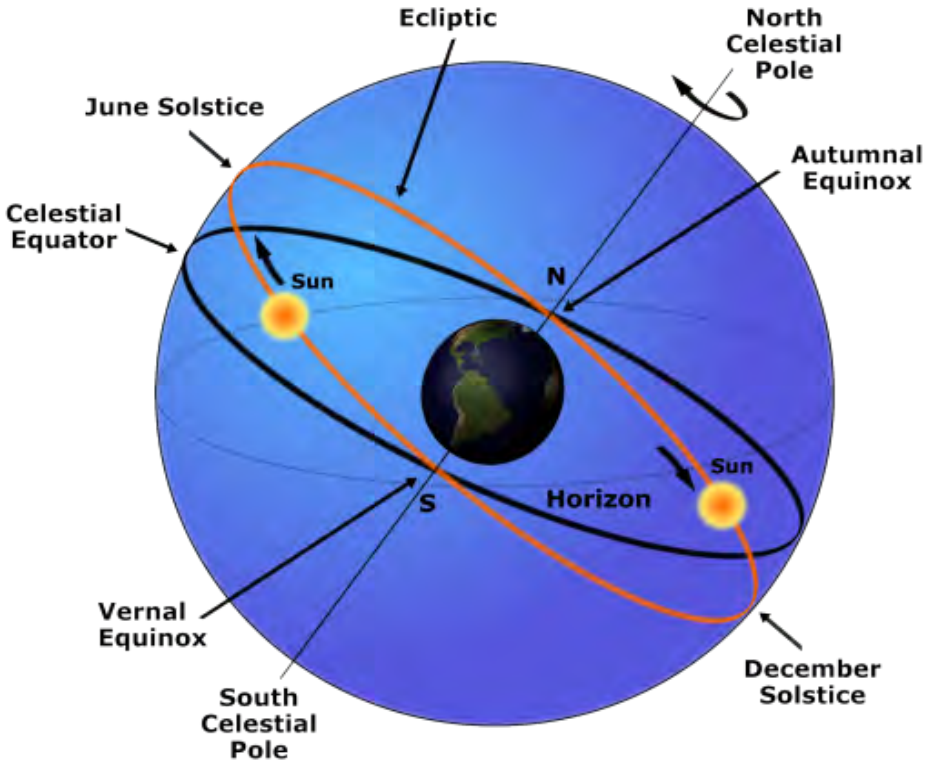

Figure 5: Sun Path orbited by the Earth. [39]

The Daylength (S_o) is the term used to describe time (in hours) between sunrise and sunset [11,22,23,33]. The duration of the Sun appearing in the sky, at a given site;

$$S_o = \frac{2\omega_s}{15}. \tag{10}$$

ETR (H_o) is a quantity that is dependent on many of these factors including; the Solar constant, the Earth's obliquity, the Solar Constant and the above mentioned solar angles [10,11,23,30,40];

$$H_o = \frac{24 \times 3.6 \times 10^{-3} I_{sc}}{\pi} \left[1 + 0.033\, cos\, \left(\frac{2\pi D_n}{365}\right)\right] \left[cos\phi\, cos\delta\, sin\omega_s + \omega_s sin\phi sin\delta\right], \tag{11}$$

The Eccentricity coefficient is defined in terms of the Earth-Sun distance [10,11,30];

$$E_o = \left[1 + 0.033\, cos\left(\frac{2\pi D_n}{365}\right)\right]. \tag{12}$$

The amount of solar radiation found at the top of the Earth's atmosphere is of great importance if we wish to predict the amount of Direct Beam Radiation incident on a horizontal surface on the Earth [10,11]. This quantity has units of energy per squared meter per day ($MJ/m^2.day$) . Understanding of the radiation lost due to scattering and reflection is also realized by studying the ETR at a particular location.

2.2.3. Measuring Solar Radiation

Knowledge of the available solar radiation in a specific site helps to better understand the nature and distribution of the incident radiation, as well as the climate in that region [31]. However, this data is not always readily available for every site on the map. Meteorological stations which measure solar radiation data and sunshine duration, often require costly equipment and high maintenance costs to record this timeously [11,31]. Most stations are too far apart and too few in numbers to establish an accurate global coverage of solar radiation information [31]. The WRC and Baseline Surface Radiation Network (BSRN), are two global networks which monitor the solar radiation received on Earth by collecting recorded data from meteorological stations across the globe. The work of these two centers serves as a reference database for solar radiation measurements in any part of the world [31]. Due to the low number of weather stations which record solar radiation data, models which are able to accurately and efficiently predict the solar radiation at a given site are constantly being studied and enhanced [11,31,41]. Some of the desired forecasting methods focus on prediction through the use of more readily available meteorological data such as air temperature, relative humidity, etc. [16,18,23].

Ground measurements of solar radiation can be conducted by using broadband instruments

which are designed to detect this electromagnetic radiation in its specific components, or by recording the sunshine duration using sun tracking devices [11,41]. Radiometry refers to the study of the measurement of electromagnetic radiation and radiometers are the devices used to carry out this task [11]. The detectors used in radiometers are of three main types; thermopile detectors, black body cavity detectors and semiconductor detectors [11].

It is important that the radiometers used to measure solar radiation at a site be calibrated against an absolute radiometer [41]. Most of these instruments consist of a thermal detector, a glass dome (protection from environmental elements), a silica cartridge (absorbs any water particles), electric circuits and a narrow aperture [11,31,41]. Thermopile detectors are able to detect radiation in the short wavelength spectrum [11]. For accurate records of measurements, these radiometers need to record data at least every hour. Older methods of solar radiation measurements include the "Burning Card Method", which works on the principle of the Campbell-Stokes sunshine recorder [11,41]. The direct beam radiation incident on this instrument is focused on a glass sphere/dome containing a card inside. The trajectory of the Sun throughout the day burns a trace onto the card. The trace on the card is then analyzed to determine the duration of sunshine as well as the time and position of the Sun at sunrise and sunset [11,41].

Pyrheliometers

These radiometers measure the Direct beam radiation incident at a specific location [11,31,41]. The detector of a pyrheliometer tracks the Sun throughout the day [11]. All radiometers consist of a thermal sensor which detects the energy of the incident radiation and converts it into electric signals [11,41]. The detection of the incident electromagnetic radiation is first conducted and then it is classified into Direct beam radiation or Diffuse radiation by analyzing the beams energy and wavelength [31,41]. Pyrheliometers disregard any of the Diffuse sky radiation whilst recording only the Direct beam radiation.

Pyranometers

Measurement of both Direct beam and Diffuse radiation is possible by using a pyranometer [11,31,41]. Some pyranometers measure only the Diffuse component by eliminating the Direct beam radiation component [41]. Pyranometers require a shading disk which is used to mask the Direct beam component in order to measure only the Diffuse sky radiation. This disk is placed over the radiometer, along the path of the Direct beam radiation [11].

It recent times, satellites have proven to be accurate in their ability to observe the solar radiation distribution along the Earth's atmosphere [31]. The images of geostationary satellites are processed to derive the solar radiation conditions at certain locations. They are also useful in monitoring and predicting the amount of cloud cover at a site [31]. Uncertainties in the measurements obtained by radiometers depend on the construction of the instrument itself. Sensitivity levels and thermal offsets are the main sources of errors [11]. Spectral effects together with meteorological factors can also play a part in any discrepancies which accompany the recordings [11,31,41]. Atmospheric parameters such as temperature fluctuations, wind and rain affect the efficiency of the radiometer, and so these errors have to be accounted for by correction methods [11,31].

2.2.4. Factors affecting Solar Radiation

ETR entering the Earth's atmosphere is depleted by processes such as absorption, reflection and scattering. [9,11,33,41,42]. Various gases, aerosols and clouds constitute the atmosphere, and each can absorb, reflect or scatter the incident radiation [9,11]. Scattering occurs according to the Rayleigh Theory of scattering and is due to the concentration of gases in the atmosphere [11]. Factors such as pollutants, aerosol concentrations, atmospheric gas concentrations and clouds convert the ETR into Diffuse Solar Radiation [9,11]. Most of these molecules can absorb the incident solar radiation or reflect it back into space.

2.2.4.1. Albedo

'Surface-Albedo' refers to the comparison of the portion of solar radiation which is reflected and back-scattered(H_R) to the incident radiation ETR (H_o) at a surface [9,11,42];

$$Albedo = \frac{H_R}{H_o}. \tag{13}$$

The H_R component is specular (uniform reflection) and diffuse (random variation in reflected rays) in nature [42]. When the incident radiation is scattered and absorbed, the variation accompanying these processes is called the 'Direct Radiative Forcing' [9].

'Cloud-Albedo' is the term used to describe the atmospheric transparency by quantifying the degree of cloudiness [9,11]. This ratio is dependent on the type of clouds and can be determined by considering the observed amount of cloud cover, sunshine duration or by computing the Aerosol Optical Thickness (AOT) of the cloud [11].

The Earth's orbit around the Sun, together with its axial spin may cause variations in the distance between the Earth and Sun, and accounts for season change, sunrise and sunset occurrences [34,42]. This astronomical effect causes a change in the amount of solar radiation

incident at a specific location, throughout the year [42]. The amount of GSR available on a surface at the Earth depends on the atmospheric conditions mentioned above. Hence, the transparency of the atmosphere (Albedo) is described in terms of aerosol and atmospheric gas concentrations [11].

2.2.4.2. Atmospheric Factors influencing the GSR

Aerosols

Aerosols are particles which are present in the atmosphere, they may be liquid or solid in nature [9]. Some of the aerosols include; dust, sulphates and carbon molecules. The aerosols can both absorb and scatter incident solar radiation. Hence, the Diffuse radiation component is increased [9,11].

Atmospheric Gases

The atmosphere is made up of air molecules and gases such as; CO_2, O_2, N_2, O, N, Ozone and Water vapor [9,11]. At certain wavelengths these atmospheric molecules absorb solar radiation. Ozone in the stratosphere absorbs UV radiation, while H_2O, CO_2, and O_2 absorb radiation in the visible and Near-Infrared regions [9]. These gases scatter solar radiation when the size of their particles is considerably small when compared to the wavelength of the incident solar radiation [9,11]. Water Vapor in the atmosphere decreases the total amount of GSR by absorbing both the Direct beam and Diffuse radiation components [11].

Clouds

Nearly 65% of the atmosphere is covered by clouds and they are perceived as regulators of solar radiation [9]. The types of clouds and their effects are detected by using meteorological satellite images [16,33]. The Cloud-Albedo effect is described as the instance when clouds reflect the incident solar radiation back into space whilst reducing the temperature of the

Earth's atmosphere [9]. If clouds completely obscure the Sun, there is no Direct beam radiation component and the total GSR is the same as the Diffuse radiation component [33]. Different types of clouds cause fluctuations in the available GSR and subsequently affect the climate experienced in a given area [9,33,41,42]. Observations (through satellite images) and models which account for the transparency, reflectivity and absorbency of the atmosphere are used together to address the effects of all factors which influence the amount of GSR received at the Earth's surface.

2.2.5. Applications of Solar Radiation

With the rapid depletion of fossil fuels, alternative renewable energy sources are greatly sought after. Solar radiation is a natural and inexhaustible source of energy. The importance of solar irradiance extends far beyond its uses in every day life, it is the primary source which allows life on Earth to exist. Along with its vital role for existence, many human and environmental processes depend on the Sun's energy for natural development. Examples of these processes include the evaporation of water which leads to precipitation, the photochemical processes involved with crop growth and the control of climatological conditions on Earth [11,43].

Radiation from the Sun can also be used directly for a number of applications such as water heating, the drying of materials, natural lighting, etc. [43]. To maximize the capability of the Sun's radiation, solar energy can be harnessed and converted into thermal and electrical energy [1,11,43]. This is accomplished by the use of solar energy conversion systems which include thermoelectric and photovoltaic (PV) technologies [11]. Collectively these are called 'Active' applications of solar radiation [1].

The first PV solar cells were invented in 1954 [1]. The evolution of this technology has

been noted over the passed few decades, with solar PV cells being more widely used due to the increase in their efficiency [44,45]. A typical PV cell is made from semiconductor material and works on the basis of the photo-electric effect [1,11]. The radiation incident on a PV cell causes electron excitation and hence a steady current which may be stored. Currently there are two types of PV cells on the market namely; Cyrstalline Silicon-based PV cells and thin film cells [1]. Semiconductor materials such as; amorphous silicon, cadmium-tellurium which are crucial for conductivity, are the dominant technologies employed in most PV cells [1]. Crystalline silicon-based PV cells are more expensive when compared to thin film cells. Their price is justified considering their vastly outperforming efficiency [1]. The energy captured by these cells is converted into electricity which is used to run appliances, for lighting purposes, and to power motors and generators [1,43]. Electricity can also be stored and used when power outages are experienced. PV systems are extremely economical in broader contexts given that their employment will aid in lowering the consumption costs of grid electricity.

Thermal electric applications involves the collection, storage and conversion of solar energy [1,11]. A solar panel consists of a large number of small PV cells connected together to increase the surface area of sunlight exposure. Large scale deployment of these solar panels in CSP's is only viable for certain areas, depending on the amount of Direct Normal Radiation received at that location [1,29]. Technologies which lend themselves to thermal electric applications in CSP's include; Parabolic troughs, solar dish collectors, Fresnel mirrors [1,46]. Fresnel Mirrors are made up of reflecting mirrors which are complexly designed to capture and store solar radiation. The mirrors are manufactured from glass which has an absorber insulation and offers a longer lifespan (more than 25 years) [46]. They are installed in parallel rows forming a horizontal layout which proves to be efficient in capturing the maximum amount of incident radiation [46].

Parabolic troughs and solar dish collectors also constitute some of these reflecting mirrors. Their design is far more complicated as the mirrors and glass are curved to form troughs [46].

These technologies can be placed at higher altitudes and therefore are affected the least by atmospheric aerosols [46]. CSP's currently use these structured devices which are efficient and economical as they have the potential to reduce the strain and costs of grid electricity [1,29,46]. PV cells find applications in both the industrial and residential sectors. These technologies are highly suitable for remote locations, which have difficulties in accessing the grid supply [44]. Solar radiation has the potential to meet the world's energy requirements through Active solar technologies such as those mentioned above.

New advances to solar cells allows for the optimal amount of radiation to be captured. Features like tracking and tilting are fitted into the solar collectors to allow them adjust to the Sun's position [43]. Placement of solar panels has direct implications on the energy output and efficiency of the panel [43]. Limitations in the application of PV cells arise from their uncertainty and variability [45]. Hence, methods to predict the amount of solar radiation incident at a given location is of great importance for the construction of PV technologies [44,45]. Accurate and efficient forecasting methods will assist in the proper placement of PV panels, customized design of these technologies and better management of grid electricity [47]. These technologies are at our disposal and can also be used in combination with the national grid supply, for example; in times of load shedding and blackouts [44,47].

Chapter 3

Literature Review

Solar radiation data is not always available for many parts of the world due to the high costs involved in its measurement, hence methods which predict solar radiation at a given location are required [16,18,48]. Precise and efficient methods of predicting solar radiation are crucial for the placement and design of solar technologies. Knowledge of the available solar radiation at a given location is also important for the management of energy resources as well as the development of these technologies [48]. Techniques used to forecast the amount of available solar resources, depend on the time scale validation of the prediction (time horizon) [49].

3.1. Forecast Horizons

Forecasting horizons describe the time interval for which values of solar radiation are predicted. The real-time acquisition of predicted data is critical for solar power plants (e.g. CSP) which supply the demand of the national grid [31,49]. Solar power plants require measuring stations to assess and forecast the incident solar radiation to allow for proper utilization of the resources [31].

Now casting

This forecasting horizon refers to predictions made in a short time interval usually between 0-3 hours [31,49]. These forecasts can be made by analyzing measurements made at a particular instant and a few hours before that instant.

Short-Term Forecasting

These forecasts are made every 3-6 hours and can be obtained by using models which incorporate meteorological data such as precipitation, wind, temperature and sunshine duration

[31,49].

Forecasting

Predictions made in the interval: 6-72 hours or longer are referred to as "forecasting". These forecasts are conducted by various techniques which include both statistical and physical approaches [31].

For accurate forecasts to be made, models which are suitable for the specific forecasting horizon are considered. (e.g. Certain Numerical Weather Prediction (NWP) Models do not perform well in Now casting, as the model may not account for variations in the meteorological conditions within the interval of 3 hours) [31,49].

3.2. Statistical Methods

Prior statistical analysis of the meteorological parameters observed in a specific location are vital for implementing modeling techniques [11]. For the prediction of solar radiation, factors such as GSR, ETR and weather parameters need to be monitored for a period of about one calendar year [11]. Satellite data (sunshine duration, cloud cover,etc.) are variables in the analysis and models used for solar radiation forecasting [11,18]. Statistical methods include; time series forecasts, Numerical Weather Prediction (NWP) Models and the use of Artificial Neural Networks (ANN). Stochastic weather models are constructed from the observed meteorological data [18]. Majority of these models require complex and tedious numerical analysis based on historical data, but are precise in their predictions [50]. Statistical research techniques and models are fast becoming the preferred method of forecasting solar radiation [11,18,48-51].

3.2.1. Numerical Weather Prediction (NWP) Models

These are mathematical models which use current weather parameters as input variables, for initial and boundary conditions [31,50]. NWP models are used to predict GSR in the 'Forecasting' horizon (Up to 48 hours), and can predict GSR on a global level [31,50]. This is referred to as General Circulation Models (GCM). For regional and local predictions, the choice of NWP depends on its efficiency, cost and accessibility to meteorological data [31]. NWP are modern and very popular methods for estimating GSR and describing the dynamics of the Earth's atmosphere, however they do require extensive computations [51].

3.2.2. Artificial Neural Networks (ANN)

Due to the intense computing power required by most statistical models of GSR forecasting, Artificial Neural Networks are used [48]. An ANN is a massive processor which works on Artificial Intelligence (AI) (mimics human intelligence) [52]. It consists of a collection of processing units which have the ability to store and process exponential data sets [52]. There are two types of ANN's namely; Multilayer Perceptron (MLP) and Radial Basic Function (RBF) [18,52]. Like other statistical methods, ANN's require the input of meteorological data. These models have a high level of accuracy and efficiency [18]. An advantage of using ANN in describing the atmosphere is its ability to accurately forecast cloud cover and formation [48]. ANN's are the future of statistical forecasting of GSR with its time saving and exponential storage capabilities [18,48,52].

3.3. Physical Models

Physical models account for the influences of the atmospheric conditions, site topography and weather conditions [11,16]. This physical approach is based largely on the processes that occur in the Earth-atmosphere system [11]. Most of these models require observed meteorological data as input variables to estimate solar radiation for a given location [51]. Some of the dependent meteorological considerations include; astronomical factors (solar constant, solar angles), physical factors (surface and cloud albedo, attenuation processes), geographical considerations (latitude and altitude of the site), and meteorological parameters (temperature, relative humidity, vapor pressure, precipitation, sunshine duration, etc.) [11,16,51]. The required meteorological parameters are available and recorded at most local weather stations or can be measured with the use of basic instruments and/or calculations. Data acquired from satellite images can be used in models which depend on atmospheric transmittance [41].

3.3.1. Sunshine Duration Models

3.3.1.1. The Angstrom Model

Sunshine duration measurement has a direct correlation to the amount of GSR incident at the Earth's surface [20-23,52]. This parameter can be considered a reliable and always available variable in the estimation of GSR [11]. The earliest known correlation of solar radiation and sunshine duration was established by Angstrom in 1924 [21]. This work is the fundamental basis of many models which are still currently used to forecast and predict solar radiation [11,17,20-23,40,50]. Angstrom recorded the incoming solar radiation data using a

pyranometer and developed the following linear relationship [21];

$$Q_H = Q_o(0.25 + 0.75)S. \tag{14}$$

Q_o represented the total incoming clear sky radiation, Q_H denoted the total incoming solar radiation, and S was the relative sunshine duration (Sunshine duration/ Maximum possible sunshine duration). Clear sky conditions were difficult to classify and define without a dependence on other factors (atmospheric, geographical, etc.) [11]. Hence, Prescott modified the Angstrom correlation by replacing the clear sky radiation with the Extraterrestrial radiation (ETR) (H_o) [11,17,50-53]. This relation became generally known as the Angstrom-Prescott relation [11,17,20-23,38,50-53];

$$\frac{H}{H_o} = a + b\left(\frac{S}{S_o}\right). \tag{15}$$

Here a, b are known as the Angstrom coefficients and $\frac{S}{S_o}$ is the relative sunshine duration.

Clearness Index (K_T)

Equation (5) represents the ratio of total incoming GSR to the incoming ETR. This is a measure of the atmosphere's transmissivity and also indicates fraction of available solar radiation at a location [40,50]. The atmosphere can be described in terms of the clearness index as in Table 1 [11];

Table 1: Classification of day type using clearness index [11].

Day Type	K_T
Clear	$0.7 \leq K_T \leq 0.9$
Partially cloudy	$0.3 \leq K_T \leq 0.7$
Cloudy	$0.0 \leq K_T \leq 0.3$

Angstrom Coefficients

The a, b coefficients in equation (15) are empirical values that are dependent on the site geography (latitude, elevation, etc.) [11,50,52,53]. These empirical values have ranges;

$0.089 \leq a \leq 0.460$ and $0.208 \leq b \leq 0.851$ for various different locations in the world [11]. The physical significance of these empirical quantities gives a partial measure of the atmosphere's transmissivity [50]. Coefficient a is a function of cloud cover, while b is the fraction by which the sky's clearness index is affected due to sunshine duration [22,50]. The relative sunshine duration $\frac{S}{S_o}$ is referred to as the 'cloud cover index' [11,50]. For days when $\frac{S}{S_o} = 1$ (clear day - no cloud cover obscuring the sun), $\frac{H}{H_o} = a + b = K_T$. The sum of the Angstrom coefficients yields the atmospheric transmittance for that day [11,50]. On overcast days $\frac{S}{S_o} = 0$, then $\frac{H}{H_o} = a$ and the clearness index is equal to the $a-$coefficient.

The Angstrom-Prescott model is noted for its high degree of accuracy in estimating GSR for many sites in the world [11,40]. Its main advantage is the requirement of just one input variable - relative sunshine duration [53].

3.3.1.2. Adaptations of the Angstrom Model

The amount of solar radiation received at any location on the Earth's surface can be accurately predicted by using measurements of short wave radiation [54]. The instruments used to capture this information are the radiometers (previously mentioned in Section 2.2.3.). Over the years, newer models which take into account the effects of various meteorological parameters, have been developed [54-57]. These parameters include; precipitation, relative humidity, dew point and air temperatures, along with sunshine duration to improve the accuracy of predictions [18,41,54,55]. These models have been derived from the fundamental Angstrom-Prescott relation, and are referred to Angstrom based relations [11]. A generalized model which was developed for world-wide use is described by [56] as;

$$\frac{H}{H_o} = 0.23 + 0.48\frac{S}{S_o}, \tag{16}$$

which uses a global average of the Angstrom coefficients.

Work done by [16], depicts an exponential relationship between the relative sunshine duration and the clearness index for Spain and is described in eq. (17). The climate in this country is considered to be similar to that of South Africa (Semi-arid and mediterranean) [16].

$$\frac{H}{H_o} = a + b\, exp\left(\frac{S}{S_o}\right). \tag{17}$$

The Angstrom coefficients are crucial for the application of the Angstrom based models. Since these coefficients are site dependent, historic solar radiation observations (for the specific site) first need to be analyzed to derive a reliable set of Angstrom coefficients [11,50,52]. An example of a model which omits the Angstrom coefficients is found in [56];

$$\frac{H}{H_o} = K\left(\frac{S}{S_o}\right)^{0.63} sin\, h^{-0.19}. \tag{18}$$

Here, the site parameters are explicitly included in the relation in the form of a zone factor (K) and the model requires the solar noon angle (h) [56].

3.3.2. Air Temperature Models

The temperature of air on the Earth's surface is directly influenced by the solar radiation absorbed in the atmosphere [54]. Measurements of solar radiation and sunshine duration are limited at many meteorological stations [18]. Areas which use recorded data from stations which are not in proximity, compromise the reliability and accuracy of the data [16,18]. This leads to the development of a model which used an easily available and measurable parameter such as air temperature [18,24-26,50]. Models which use air temperature as a parameter to predict GSR at a location, require measurements of maximum and minimum air temperatures depending on the forecast horizon [11,16,18].

3.3.2.1. The Hargreaves-Samani (H-S) Model

Limitations in the availability and accessibility of solar radiation data resulted in the air temperature approach which was developed by Hargreaves and Samani [26]. The main assumption of this model is that the GSR at a site is responsible for the temperature range [16]. The difference in the daily measured maximum and minimum air temperatures are related to the amount of GSR received by the following equation [24,26];

$$H = H_o \, K_r \, (TR)^{0.5}, \tag{19}$$

where K_r is an empirical coefficient that is dependent on the site and various meteorological parameters [25], and TR refers to the difference between maximum and minimum temperatures ($TR = T_{max} - T_{min}$).

This model allows for solar radiation estimation through use of minimal meteorological data and is advantageous for locations where availability of meteorological data is limited. However, the risks associated with implementing this model lie in the assumption that the extraterrestrial and global solar radiation values are directly related to the air temperature difference [24]. For a specific location, significant errors may arise due to the influences of various other factors (elevation, storm patterns, cloudiness, humidity, advection) on the air temperature [24,25].

Empirical coefficient K_r

Studies conducted in [25,26] indicate that the value of the empirical coefficient K_r in the H-S equation depends on the location's site, humidity as well as its geographical situation with respect to large masses of water (lakes, dams, oceans). For inland / interior regions, the recommended value of K_r is 0.162, while for coastal regions $K_r = 0.19$ [16,18,24-26,58,59]. A location is classified as coastal if the location is situated on or close to the coast (interaction between land and sea) [25]. The effects of relative humidity, pressure and cloudiness were

investigated to recalibrate the value of K_r , but diverted the equation from its simplicity and main purpose [25,59,60]. Further studies resulted in a temperature dependent equation for the estimation of this empirical coefficient [24,47,58];

$$K_r = 0.00185(TR)^2 - 0.0433(TR) + 0.4023\,. \tag{20}$$

The HS relation implicitly accounts for the relative humidity at a site in the temperature range (TR) [18,24-27,58,60]. The evaluation of this empirical coefficient is solely based on the temperature difference. If the air temperature if affected by other climatic factors such as; location topography, elevation, proximity to a large body of water, then the K_r coefficient has to be corrected to avoid errors [24,25]. To address the effects of proximity to a large body of water and elevation effects, equations for the empirical coefficient are defined below in terms of the atmospheric pressure$P$ of a location and the atmospheric pressure at sea levelP_o [24,25];

$$K_r = 0.17\frac{P}{P_o} \qquad Interior \tag{21}$$

$$K_r = 0.2\frac{P}{P_o} \qquad Coastal \tag{22}$$

3.3.2.2. Combination Models

Physical methods used to predict solar radiation data at a specific location, largely depends on the meteorological data available [18,55,56]. Models which incorporate measurements of sunshine duration, air temperature and relative humidity are known as combination models [16,23,44,55,61]. Humidity is defined as the amount of water vapor present in the air, and is determined by the air temperature [41,55]. Relative humidity (R) is expressed as a percentage and reaches a daily minimum around midday (solar noon) and a maximum at

sunrise [55]. The development of models which correlate more than one variable are highly dependent on the site of interest [23,55,61]. Nigeria is found in the Northern Hemisphere and has a tropical climate with high rainfall in the summer season [23]. South Africa also experiences similar climatic conditions, and in particular KwaZulu-Natal. [23] proposed the following linear model for estimating the average monthly GSR in Nigeria;

$$\frac{\bar{H}}{\bar{H}_o} = 1.387 + 1.592\frac{\bar{S}}{\bar{S}_o} - 0.045\bar{T_m} + 0.004\frac{\bar{R}}{100}, \tag{23}$$

Here $\bar{T_m}$ is the average daily maximum temperature and $\bar{R}$ is the average daily relative humidity [23]. These combination regression equations were found to have a higher correlation when compared to models using just one meteorological variable [23,55,61].

Chapter 4

Method and Materials

4.1. Experimental Technique

Details of the geographical location of Pietermaritzburg and the three suburbs considered for this study (Northdale, Scottsville, Bisley) are presented in Chapter 6, Table 1. Daily maximum and minimum temperatures were measured and recorded using a Major Tech - MT668 Temperature and Humidity Data Logger. These values were recorded between daily, sunrise and sunset intervals. The measurement intervals were controlled and set to record every 2 hours. The sensors were calibrated at 1.5m above the ground in unshaded, open areas for each of the towns. Air temperature data was downloaded and stored monthly. The Agricultural Research Council (ARC) provided measured daily GSR and monthly sunshine duration values to the research center in Ukulinga, Bisley. These measurements served as our experimental values ($H_{measured}$), for comparison (Refer to Appendix B for set of daily results). Due to the extensive computations, a fortran program was developed to compute the daily H, H_o, S_o, K_T values, using equations (5,7,8,10-12,19) and by inputting the D_n, ϕ, $T_{max}\,T_{min}$ (Refer to Appendix A). The empirical coefficientK_r was calculated for Bisley using the provided data in equation (20). Linear correlations between the clearness index K_T and the relative sunshine duration $\frac{S}{S_o}$ were used to determine the Angstrom coefficients according to equation (15). The method used to determine these coefficients is described in Figure 6 ,below.

Calculated values of H for each of the towns were compared to the measured values provided by the Ukulinga Research Center ($H_{measured}$). The Root Mean Square Errors (RMSE) were computed for the monthly averages (Refer to Chapter 6). To determine the degree of correlation for the relative sunshine duration and clearness index, the Pearson correlation

coefficient (r) was calculated for the three regression equations obtained.

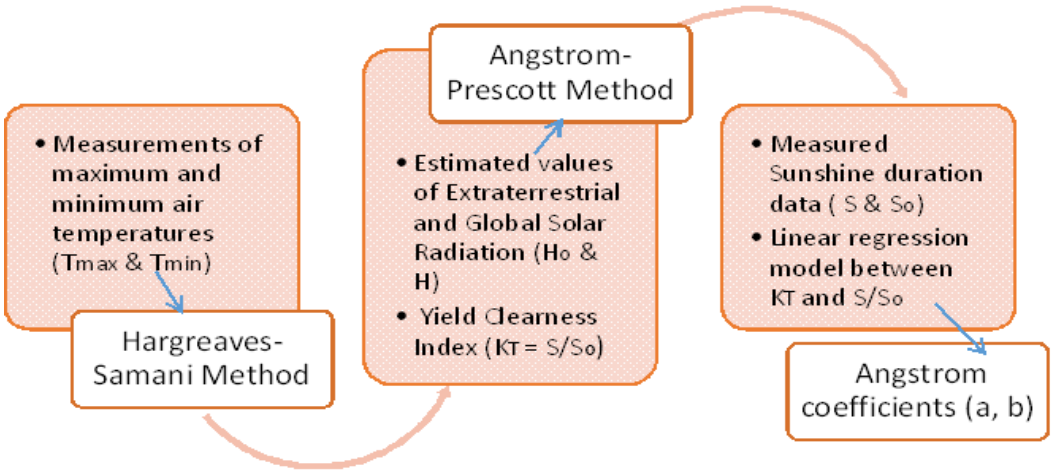

Figure 6: Flow diagram indicating method for calculating the Angstrom coefficients.

Our work was limited by the availability of solar radiation and sunshine duration data for this city. Local weather stations including, the South African Weather Services (SAWS) were unable to provide the necessary data because such recordings are not conducted in Pietermaritzburg. We did not account for the erratic weather conditions (wind, rain) that are experienced in Pietermaritzburg. The time frame for this study was hindered by the late arrival of equipment and data, hence a study period of one calendar year was chosen, as opposed to one Julian year.

Chapter 5

Results and Discussion

Graphical representations of the results obtained in this study for July 2014 up to and including June 2015, are represented in Chapter 6, while detailed daily measurements and calculations are provided in Appendix B.

The maximum and minimum temperature fluctuations monitored for the three cities are illustrated in Figures: 2 and 3 in Chapter 6. The measured maximum and minimum temperatures were used to compute the GSR values for Northdale, Scottsville and Bisley according to the H-S equation (eq. (19)). Due to the subtropical and semi-arid climate of KwaZulu-Natal, moderately warm temperatures are experienced throughout the year. Maximum temperatures were observed in the summer months (December - February). Annual average measurements of the maximum and minimum temperatures are provided in Figures 7 and 8 below.

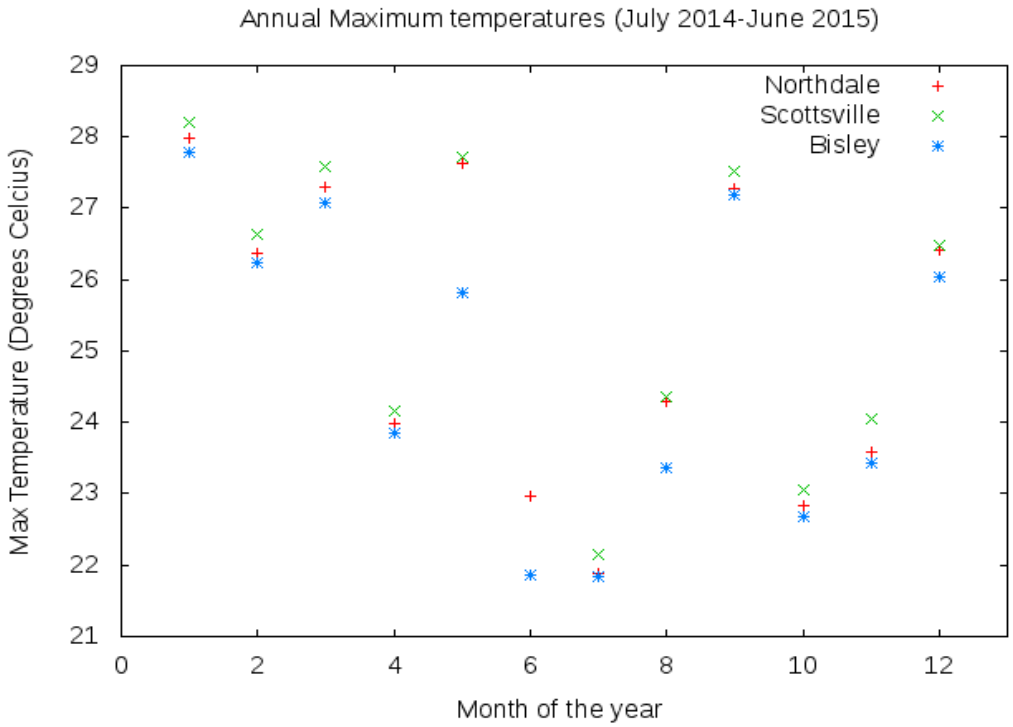

Figure 7: Average maximum temperatures for the year.

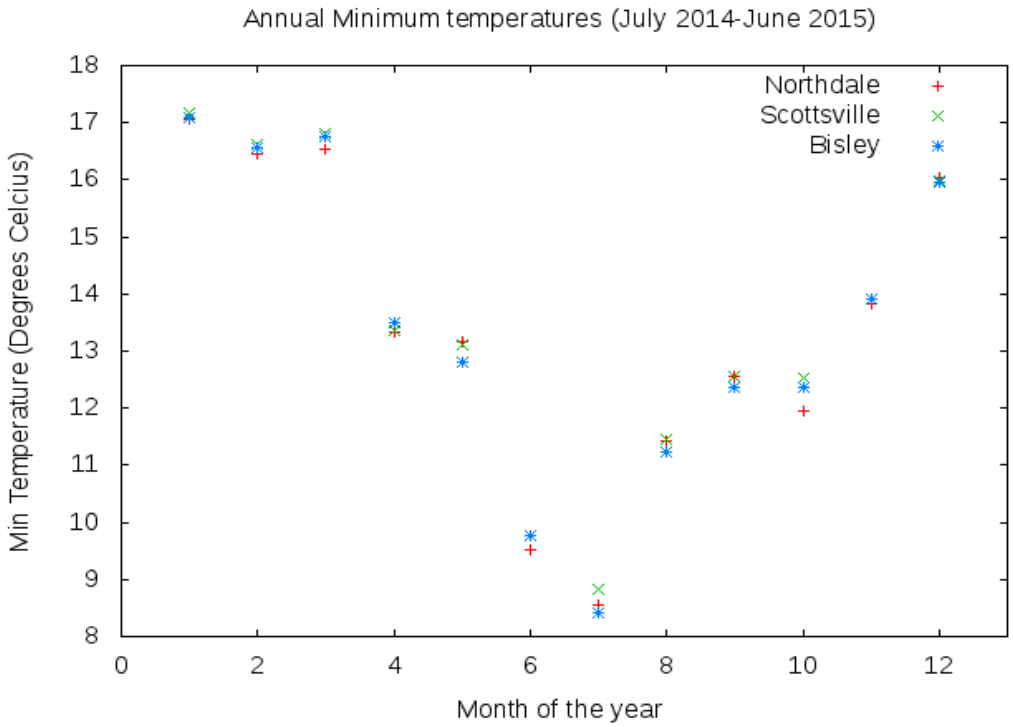

Figure 8: Average minimum temperatures for the year.

For all suburbs, the daily minimum temperatures were observed close to sunrise (between 05:00 am and 07:00 am), when the percentage relative humidity was higher. While the daily maximum air temperatures were observed around midday (between 11:00 am and 13:00 pm), when the percentage relative humidity was lowest. The average measured maximum temperatures in Bisley are lower than those of Northdale and Scottsville (Figure 7), this explains the variations in the calculated values (H_N, H_S) when compared to H_B .These differences may be due to the land use and elevation of this suburb. Despite the proximity of the chosen sites, large temperature variations were incurred. The cheap equipment used to measure the air temperature data may have contributed to the poor recordings, as the equipment may have deteriorated over time. Since the land use in Bisley is more industrial, pollutants and aerosols will have a greater effect on the GSR estimates for this site. Air temperature measurements and calculated GSR values for Northdale and Scottsville are much higher than those for Bisley. The differences in the land use, latitude and elevation of these three suburbs influences both the temperature measurements and GSR results.

Daily calculated values of H (H_N, H_S, H_B) show close coherence to the $H_{measured}$ values provided by the ARC, this is shown in Figures 4,5 and 6 in Chapter 6. The distribution of the calculated GSR values in Pietermaritzburg show seasonal variation, with the highest records being observed in the spring and summer months (October - February). A decline in the annual average GSR values is visible in the winter months (June - August) (Refer to Figure 7, Chapter 6). During November - January, the H values predicted by the H-S equation are higher than the actual observed GSR measurements. These variations may be explained by the temperature variations in Bisley as compared to Northdale and Scottsville. Other meteorological factors such as wind speed, rainfall and climate may influence these values and our model does not fully accommodate for these parameters. Most of the rainfall experienced in South Africa, occurs during the summer months. The overall annual distributions of the average GSR values conform to a similar shape, with peaks around December

and January with the lowest values found in June. In comparison to the study conducted in [58], for a site which has a similar climate and latitude to that of Pietermaritzburg, the annual average GSR range for Pietermaritzburg showed fair agreement to the annual average observed H values for the Limpopo Province.

Average monthly results are presented in Tables 2,3 and 4 in Chapter 6. The empirical coefficient K_r was calculated using the Bisley data and results are listed on Table 4, Chapter 6. These calculated values were inconsistent throughout the year and could not be used in the Hargreaves Samani model. The differences could be due to a number of effects on the temperature data such as; cloudiness, relative humidity, wind speed, advection. By analysing data from a number of years it would be possible to estimate a value for K_r for Pietermaritzburg. In our work we have used the suggested value for the empirical coefficient $K_r = 0.162$ since Pietermaritzburg is an inland region. The Root Mean Square Errors were computed for the monthly average calculated (H_N, H_S, H_B) values and measured values (H_{meas}) , with the largest annual average error being 4.52 in the Scottsville results for July 2014- June 2015. The HS model proved to be accurate in estimating the amount of GSR received in the three suburbs for most of the year, with shortfalls occurring in the summer season.

Linear correlations were used to graph the clearness index (K_T) against the relative sunshine duration ($\frac{S}{S_o}$) in order to determine the Angstrom coefficients according to eq. (11). The monthly average values of H and H_o for the three suburbs were used as only the monthly values of S were available. Monthly average results are provided in Tables; 2, 3 and 4 in Chapter 6. A linear fit was used and plotted in Figures; 8, 9 and 10, and the Angstrom coefficients obtained are listed in Table 6 in Chapter 6. The regression equations derived from these Angstrom coefficients for Northdale, Bisley and Scottsville are as follows;

$$\frac{H_N}{H_{o_N}} = 0.26 + 0.39\frac{S}{S_{o_N}} \tag{24}$$

$$\frac{H_S}{H_{o_S}} = 0.23 + 0.41\frac{S}{S_{o_S}} \tag{25}$$

$$\frac{H_B}{H_{o_B}} = 0.24 + 0.40\frac{S}{S_{o_B}} \tag{26}$$

From the monthly averages each of the three cities experienced mostly 'partially cloudy' days throughout the year as classified by Table 1. These are days which have a clearness index in the following range; $0.3 \leq K_T < 0.7$. Cloudiness has a direct effect on the air temperature and hence the solar radiation values. Clouds absorb and reflect incoming solar radiation and therefore decrease the H_o. This may have been the main source of errors for the differences in measured and calculated values of H. Measurements taken on clear sky days would give a more accurate description of the available global solar radiation. While other atmospheric factors such as pollutant and aerosol concentrations may have also contributed to the errors in the calculated ETR and GSR values. For May 2015, there are no 'clear sky' days from the data provided, however our measurements and calculations show four 'clear sky' days observed for both Northdale and Scottsville. The geographical factors and land use difference between the sites may play a role in this difference in the calculated number of 'clear sky' days. Bisley is an Industrial zone and has higher concentrations of pollutants and aerosols in the atmosphere as opposed to Northdale and Scottsville. The errors in the calculated GSR and ETR values arise from the effects of all the factors mentioned above which influence solar radiation, and result in errors in calculated values of K_T. With the calculated Angstrom coefficients, the Angstrom-Prescott model can be seen as a second simple method of estimating the GSR incident in Pietermaritzburg, which requires only one input parameter i.e. relative sunshine duration. The coefficients produced by our estimated values of GSR can be enhanced by the analysis of historic GSR data for Pietermaritzburg, since these coefficients are highly dependent on the site of interest. We then proceeded to determine the degree of linear correlation for the average of these equations, by calculating the Pearson correlation coefficient (r). A moderate linear relationship between the estimated clearness index and relative sunshine duration was described by a correlation coefficient of $r = 0.583$. This is a

comparatively low coefficient of determination with regards to work conducted in [21,22,60], whose study period was more than one year.

Conclusion

Pietermaritzburg receives ample sunshine throughout the year, which can be harnessed and used in solar thermal and PV applications. Though this city is not suitable for the construction of a CSP, small scale solar PV cells are a viable option for the industrial and residential sectors. With the current energy status in South Africa, businesses are forced to halt work during power outages and this has had devastating consequences on the economy. Solar cells can be employed as back up sources of energy for businesses as well as to supplement the grid power supply. This will alleviate the strains placed on non-renewable resources such as coal and liquified petroleum. Solar energy is a safe and unlimited energy source, which will also aid in reducing the country's carbon footprint.

The data logger sensor used in this study, was able to monitor temperature and humidity fluctuations efficiently and timeously. This device served as a cheap and easily accessible method of measuring these weather parameters. The Hargreaves-Samani (H-S) model proved to be a reliable method for estimating the amount of GSR in Pietermaritzburg, but lacked accuracy during the rainy summer season. Our model can be modified to account for other meteorological parameters such as rainfall, relative humidity and wind speed, which may have been the cause of the discrepancies in our calculated GSR values. The H-S equation is simple and can be adopted for use in any geographical location.

Further studies within this work would include constructing a linear combination model which allows for variations in wind speed, rainfall, sunshine duration and relative humidity. For this one would need a cost efficient and easy to implement method of measuring precipitation and wind speed in this city, as weather station records are limited. Further-

more, for areas where meteorological data such as solar radiation are missing, the H-S model can be applied by weather stations to provide estimates of the required data. With the aid of the internet, access to this information can be made readily available, and on a global scale.

Design and placement of PV technologies such as solar panels can be enhanced by these GSR predictions, however this is not the only advantage of GSR knowledge of a location. Solar radiation data is vital for the interpretation of climate and global warming effects for a given location, along with many other applications.The Angstrom-Prescott model allows for a second simple and efficient method of estimating GSR within any geographical location, provided sunshine duration data is available. Establishing a set of reliable Angstrom coefficients is vital for use of this model and requires consideration of historic solar radiation data for the given site. A study period of about 10 years is prescribed for obtaining a strong set of coefficients. This model can also be used by weather stations to predict GSR for sites where this data is too costly to record.

References

[1] Govinda R. T., Lado K., Patrick A. N. A review of solar energy, markets, economies and policies. Policy research working paper. The world bank, development and research group, environment and energy team. 2011. Available from: http://econ.worldbank.org

[2] ESKOM web page [Internet]. Available from: http://www.eskom.co.za/AboutElectricity/ElectricityTechnologies/Pages/Coal_Power.aspx

[3] Renewable Energy| Department: Energy| Republic of South Africa [Internet]. Available from: http://www.energy.co.za/files/esources/renewables/r_solar.html

[4] Winkler H. Energy Policies for sustainable development in South Africa. Energy for Sustainable Development. Vol. XI (1). 2007.

[5] Trollip H., Butler A., Burton J., Caetano T., Godinho C. Energy Security in South Africa. Mitigation Action Plans and Scenarios. Cape Town. Issue no. 17. 2014

[6] Fourteenth Session of the United Nations Commission on Sustainable Development. South Africa country report. Department of Environmental Affairs and Tourism. 2005.

[7] Letete T., Guma M., Marquard A. Information on climate change in South Africa: greenhouse gas emission and mitigation options. University of Cape Town. Energy Research Center. 29pp. 2009.

[8] Davis C. L. Climate risk and vulnerability. A handbook for Southern Africa. Council for Scientific and Industrial Research, Pretoria, South Africa. 2011. pp. 92. ISBN: 978-0-620-50627-4

[9] Qiang Fu. Radiation (Solar). University of Washington. Seattle, WA. USA. Elsevier Ltd. 2003

[10] Sayigh A. A. M. Solar radiation availability prediction from climatological data. Academic Press, New York. 1977. pp.61. ISBN: 0-12-620850-6

[11] Viorel B. Modeling solar radiation at the earth's surface: Recent advances. Springer. 2008. ISBN: 3540774548

[12] Earth System Science Education Alliance (ESSEA), Institute for Global Environmental Strategies (IGES) [Internet]. Image provided by the National Science Digital Library. 2015. Available from: http://esseacourses.strategies.org/module.php?module_id=99

[13] Boeker E., Van Grondelle R. Environmental physics: Sustainable energy and climate change. 3rd Ed. John Wiley and Sons Ltd. 2011.

[14] Kennewell J. Mc Donald A. IPS-Satellite communications and space weather [Internet].The Australian Space Weather Agency. 2008.
Available from: http://www.ips,gov.au/Educational/1/3/2

[15] Queener B. D. Intra-hour direct normal irradiance solar forecasting using genetic programming. [Electronic Masters Thesis]. San Diego, California, USA. 2012. Available from: http://escholarship_uc_item3g06n4dp.pdf

[16] Almorox J., Hontoria C., Benito M. Models for obtaining daily global solar radiation with measured air temperature data in Madrid (Spain). Applied Energy 88. 2011. pp.1703-1709. DOI: 10.1016/japenergy.2011.11.003

[17] Tijjani B.I. Comparison between first and second order Angstrom type models for sunshine hours in Katsina Nigeria. Bayero Journal of Pure and Applied sciences. Vol 4(2). pp.24-27. Available from: dx.doi.org/10.4314/bajopas.v4i2.5

[18] Rahimikoob A. Estimating global solar radiation using ANN and air temperature data in semi-arid environment (Iran).
Renewable Energy. Vol. 35. 2010. pp.2131-2135. DOI:10.1016/j.renene.2010.01.029

[19] Al Riza D. F., Gilani S. I., Aris M. S. Hourly solar radiation estimation using ambient temperature and relative humidity data. International Journal of Environmental Science and Development. Vol. 2(3). June 2011.

[20] Gadiwala M. S. Usman A., Akhtar M., Jamil K. Empirical models for the estimation of global solar radiation with sunshine hours on horizontal surface in various cities of Pakistan. Pakistan Journal of Meteorology. Vol. 9(18). 2013.

[21] Angstrom A. Solar and atmospheric radiation. International commission for solar research on Actinometric Investigations of solar and atmospheric radiation. Journal of the Royal Meteorological Society. pp.121-126. 1923.

[22] Srivasta R. C., Pandey H. Estimating Angstrom-Prescott coefficients for India and developing a correlation between sunshine hours and global solar radiation for India. ISRN Renewable Energy. Vol 2013. Hindawi Publishing. Available form: http://dx.doi.org/10.1155/2013/403742

[23] Ituen Eno E., Esen Nisken U., Nwokolo Samuel C., Uto Ema G. Prediction of Global solar radiation using relative humidity, maximum temperature and sunshine hours in Uyo in the Niger delta Region, Nigeria. Advances in Applied Science Research. Vol. 3(4). 2012.

pp.1923-1937. ISSN: 0976-8610

[24] Samani Z. Estimating solar radiation and evapotranspiration using minimum climatological data. Journal of Irrigation and Drainage Engineering. 2000. pp.265-267.

[25] Allen R.G. Self-calibrating method for estimating global solar radiation from air temperature. Journal of Hydrologic Engineering. New York. Vol.2. 1991. pp.56-57. ISSN: 10840699

[26] Hargreaves G. H., Samani Z. A. Estimating potential evapotranspiration. Journal of irrigation and drainage engineering. ASCE. 108(IR3). 1982. pp.223-230.

[27] Diabate L., Blanc P., Wald L. Solar Radiation climate in Africa. Solar Energy. No. 76. Elsevier Ltd. pp.733-744. 2004. <hal-00361362>

[28] Thornhill M., Green-Govender J., Khoza B. A Status Quo analysis on the impacts of climate change in KwaZulu-Natal. Report to the department of Agriculture and Environmental Affairs. Provincial Government, KwaZulu-Natal, South Africa. 2009.

[29] Fluri T. P. The potential of Concentrating Solar Power in South Africa. Energy Policy. No. 37. pp.5075- 5080. 2009.

[30] Iqbal Muhammad. An Introduction to solar radiation. Elsevier Ltd. 2012.

[31] Palescu M., Palescu E., Gravila P., Badescu V. Weather modeling and forecasting of PV systems operation. Springer Science and Business Media. 2012.

[32] Boyle G. Renewable Energy. OXFORD University Press. 2004.

[33] Campbell G. S., John M. N. An Introduction to environmental biophysics. 2nd Ed. Springer, New York. 1998.

[34] Sproul A. B. Derivation of the solar geometric relationships using vector analysis. Renewable Energy. No. 32. pp.1187-1205. 2007.

[35] Conradie D. Maximising the Sun. 2010.

[36] Roderick M. L. Methods for calculating solar position and day length included computer programs and subroutines. Land Management, Western Australian Department of Agriculture. 1992.

[37] Meinel A. B., Meinel M. P. Applied solar energy. An Introduction. 1976.

[38] Wayfinding: Modern Methods and Techniques of Non-Instrument Navigation, Based on Pacific Traditions. The Polynesian Voyaging Society. Voyage into the New Millennium. Hana Hou, 41.

[39] The poetics of daily life in America. [webpage]. Available from: http://poetics-ray.blogspot.com

[40] Salima G., Chavula G. M. S. Determining Angstrom coefficients for estimating solar radiation in Malawi. International Journal of Geosciences (3). pp. 391-397. 2012.

[41] Gilani S. I. U. H., Dimas F. A. R., Shiraz M. Hourly solar radiation estimation using ambient temperature and relative humidity data. International Journal of Environmental Science and Development, 2(3). pp. 188-193.

[42] E. B. Babatunde. Solar Radiation, a friendly renewable energy source. INTECH Open

Access Publisher. 2012.

[43] Dresselhaus M. S., Thomas I. L. Alternative Energy Technologies. Nature, 414 (6861). pp. 332-337. 2001.

[44] Kumar R., Umanand L. Estimation of global radiation using clearness index model for sizing PV systems. Renewable Energy, 30. pp. 2221-2233. 2005.

[45] Pelland S., Remund J., Kleissl J., Oozeki T., De Brabandere K. Photovoltaic and solar forecasting: State of the art. IEA PVPS. Task 14. 2013.

[46] Pitz-Paal. Concentrating Solar Power. Energy: Improved, Sustainable and Clean Options for our planet. Elsevier, Oxford. pp. 171-192. 2008.

[47] Ulbricht R., Fischer U., Lehner W., Donker H. First steps towards a systematical optimized strategy for solar energy supply forecasting. In proceedings of the European Conference on Machine Learning and Principles and Practice of Knowledge Discovery in Databases (ECMLPKDD). Prague, Czech Republic, Vol. 2327. 2013.

[48] Kiehl J. T., Hack J. J., Bonan G. B., Boville B. A., Williamson D. L., Rasch P. J. The National Center for Atmospheric Research. Community Climate Model: CCM3*. Journal of Climate, vol. 11 (6). pp. 1131-1149.

[49] Zhang J., Hodge B. M., Forita A., Lu S., Hamann H. F., Banunarayanan V. Metrics for evaluating the accuracy of solar power into power systems, London, England.

[50] Sendanayake S. Miguntanna N. P., Jayasinghe M. T. R. Estimating incident solar radiation in tropical islands with short term weather data. European Scientific Journal, vol. 10

(3). 2014.

[51] Abraha M. G., Savage M. J. Comparison of estimates of daily solar radiation from air temperature range for application in crop simulations. Agricultural and Forest Meteorology, 148. pp. 401-416. 2008.

[52] Prescott J. A. Evaporation from water surface in relation to solar radiation. Transactions of the Royal Society of Australia, 46. pp. 114-118. 1940.

[53] Teke A., Yilidirim H. B. Estimating the monthly global solar radiation for Eastern Mediterranean Region. Energy Conversion and Management, 87. pp. 628-635. 2014.

[54] Allen R. G., Pereira L. S., Raes D., Smith M. Crop Evapotranspiration (Guidelines for computing crop water requirements). FAO Irrigation and Drainage Paper No. 56. 2006.

[55] Falayi E. O., Adepitan J. O., Rablu A. B. Empirical models for the correlation of global solar radiation with meteorological data in Iseyin, Nigeria. International Journal of Physical Sciences, vol. 3 (9). pp. 210-216. 2008

[56] Page J. K. The estimation of monthly mean values of daily total short wave radiation on vertical and inclined surfaces from sunshine records for latitudes 40^oN - 40^o S. In : Proceedings of UN conference on new sources of energy. pp. 378-390. 1961.

[57] Chegaar M., Chibani A. A simple method for computing global solar radiation. Rev. Energy. Ren. : Chemss. pp. 111-115. 2000.

[58] Maluta E. N., Mulaudzi T. S., Sankaran V. Estimation of the global solar radiation on the horizontal surface from temperature data for the Vhembe District in the Limpopo

Province of South Africa. International Journal of Green Energy, 11 (5). pp. 454-464. 2014.

[59] Hargreaves G. H., Allen R. G. History and evaluation of the Hargreaves evapotranspiration equation. Journal of Irrigation and Drainage Engineering, 129 (1). pp. 53-63. 2003.

[60] Raziei T., Pereira L. S. Estimation of ETo with Hargreaves-Samani and FAO-PM temperature methods for a wide range of climates in Iran. Agricultural Water Management, 121. pp. 1-18. 2013.

[61] Waleed I. Empirical Models for the correlation of clearness index with meteorological parameters in Iraq. IOSR. Journal of Engineering, 4 (3). pp. 12-18. 2014.

CHAPTER 6

RESEARCH ARTICLE

Submitted to journal titled: Renewable Energy, Elsevier Ltd. Currently under review.

Quantifying the global solar radiation received in Pietermaritzburg, KwaZulu-Natal by using a temperature based method (Hargreaves-Samani) to determine the Angstrom coefficients through the clearness index.

Tamara Rosemary Govindasamy[1], Naven Chetty*[1,2]

1. University of KwaZulu- Natal, School of Chemistry and Physics, 2. Author for correspondence: chettyn3@ukzn.ac.za

Abstract

Power outages and scheduled load shedding has become a part of every South African citizens daily routine. With the increase in cost of conventional energy sources, and the depletion of fossil fuels, attempts to use renewable resources to their full potential are underway. South Africa and in particular Pietermaritzburg receives sunshine throughout the year, making it very suitable for harnessing solar power. In this work we forecast the amount of Global Solar Radiation (GSR) received in three different suburbs in the city of Pietermaritzburg. Pietermaritzburg is the capital of the KwaZulu-Natal province. The primary aim of this study is to determine which areas are most suitable for the use and implementation of photovoltaic technologies. An air temperature model (Hargreaves-Samani model) is used to forecast the global solar irradiance received in these locations for a period of one calendar year, as solar radiation data is not readily available within the city. We proceed to determine the Angstrom-Prescott coefficients for the city, from the obtained monthly clearness index. This served as a second simple method of forecasting the solar radiation by using the sunshine duration. Our results compare fairly well with the observed data provided by the ARC, with an average annual RMSE of 4.52 and an average annual difference in monthly values of GSR not

exceeding 1.99 MJ/m^2. The Angstrom coefficients for the year studied, result in values of a=0.24±0.07 and b=0.40±0.06. Though Pietermaritzburg may not be suitable for large scale solar power plants, the employment of solar panels in both industrial and residential areas will contribute greatly to a decrease in demand of grid electricity.

Keywords; Load shedding, Global solar radiation, Photovoltaic technologies, Air temperature model, Angstrom coefficients.

Introduction

Solar energy is a pure, inexhaustible, and readily available resource. The increase in price of conventional energy sources, together with the depletion of non-renewable resources and fossil fuels, necessitates a great demand for alternative power sources. Green energy sources which are beneficial to the environment, are being studied as alternate resources which could potentially aid in the energy crisis. The cost of these technologies has reduced significantly in the past decade, however it still remains higher than the cost of conventional energy and hence uptake is still relatively slow [1].

Within South Africa, we rely solely on the energy harnessed from coal power stations operated by ESKOM, the state power utility. The increased demand for electricity has resulted in an increase in production costs due to the strain placed on existing power stations, aging infrastructure as well as the depletion of non-renewable resources [2]. Since our country has been alarmed about the security of energy resources for the country's power needs, load shedding (power outages) have been implemented almost daily in a bid to save energy [2]. The consequences of load shedding has affected the entire country with even more devastating effects on the economy [2,3].

Growth in solar energy technologies has been noted, together with its theoretical potential

to supply the global demand for energy being the major contributing factor [1]. South Africa is well suited for the harnessing of solar radiation because sunshine is available throughout the year including the winter months. Depending on the geographical location certain areas in Africa receive more than double the amount of radiation as compared to countries in the northern hemisphere [3]. Despite this abundance, there are many financial and technical restraints with regards to solar energy technologies, which limits its use to private off-grid connections. These limitations need to be overcome in order to increase the contribution of solar power to the energy supply of the country.

The amount of solar radiation incident at the earth's surface is a measurable quantity. Solar radiation outside of the earth's atmosphere, received at a surface which is normal to the incident radiation is known as the solar constant [4,5]. This quantity is measured from space through the use of satellite data and has a value of 1367 Wm^{-2}, which changes by approximately 0.01% over a period of 30 years [5-8]. The amount of solar radiation received at the earth's surface is largely depleted due to the attenuation processes which occur in the atmosphere [6].

Solar radiation is responsible for many processes which occur on the earth's surface and its research finds applications in many science and engineering fields [9]. Knowledge and prediction of solar radiation available at a specific location is of great importance for the designing and performance evaluation of solar energy conversion systems [9,10]. Solar energy can be harnessed and utilized for applications which fall into two main categories; Solar Thermal and Solar Photovoltaic (PV) [1, 9,10].

In many geographical locations, Global Solar Radiation (GSR) is not measured because it is too expensive to purchase and maintain the apparatus required. If measured data is available it is not always complete as equipment can fail due to numerous faults [9,11]. As a result, accurate and efficient forecasting methods are increasingly required. Hence researchers have

employed the use of empirical methods which are able to calculate and predict GSR for a particular location [5,9,11-13].

Many of these empirical models require the input of other meteorological variables (which are often more readily available than solar radiation data) or historical weather data. Some of these meteorological parameters include; air temperature, precipitation, relative humidity, sunshine duration, etc. [11-13]. The empirical model is classified according to the climatic variable which it requires [9], e.g. sunshine duration models [10,13-16], temperature based methods [9,17-19], and cloud-based methods which require the use of satellite sky images [6].

Sample Site Details

The city of Pietermaritzburg (Midlands) is the capital city in the KwaZulu-Natal province in South Africa. This city is found in a hollow which is surrounded by the escarpment (Drakensberg Mountain Range) and is seen as an inland region. Having a geographical location that ideally receives sunshine throughout the year, Pietermaritzburg is one of the warmest cities in the province. Three towns in this city were chosen for the study; Northdale, Scottsville, and Bisley. Northdale is considered a residential area as there are no major industrial/ commercial enterprises. Table 1 provides the geographical data of the three chosen sites. The land use in Scottsville is dense commercial and mixed residential, especially surrounding the University of KwaZulu-Natal, while Bisley has more of an industrial and commercial settings. Figure 1 is an image of Bisley, Pietermaritzburg. Weather stations in the neighboring cities did not have records of daily solar radiation or sunshine duration for Pietermaritzburg. Such data is not readily available for this location, hence making this work very important as a predictor of GSR. A study center in Ukulinga (Bisley, Pietermaritzburg), was able to provide the necessary data required for this work. Temperature, Humidity and Dew point measurements were recorded hourly with the use of a sensor.

The main focus of our research was to predict the amount of global solar radiation received in Pietermaritzburg using meteorological data that was readily and easily available. Since the cost of equipment to measure certain climatic parameters was too high, we decided to use an approach that estimated solar radiation using air temperature. Records of solar radiation incident in Pietermaritzburg are conducted by the Agricultural Research Council (ARC). The ARC conducts work with the Ukulinga Research Center (based in Bisley), and was able to provide the necessary GSR data for Bisley. This data was used to verify our calculations and interpret our differences. The Hargreaves-Samani equation [19] was used to calculate the solar radiation incident on a horizontal surface, for each town following the approach studied by Maluta et al. [20]. Thereafter we proceeded to calculate Angstrom coefficients for our city from the GSR data we collected over the year. Due to time and equipment constraints we were only able to take measurements over a period of one calendar year, however this technique can be used to analyze historic data for any location.

Table 1: Geographical details of study sites

	Northdale	Scottsville	Bisley
Latitude ϕ (South)	-29.551^0	-29.617^0	-29.668^0
Longitude (East)	30.395^0	30.397^0	30.416^0
Elevation	753m	632m	752m

Background Theory

In areas where solar radiation information is not readily available, methods of forecasting are employed. The simplest method involves the use of the air temperature of a given location. Air temperature measurements are easy to conduct and can be obtained in regions where there are no weather stations nearby. The Hargreaves-Samani equation [18-20] relates the amount of extraterrestrial radiation (H_o) to the difference between the maximum and minimum air temperatures ($TR = T_{max} - T_{min}$), in order to calculate the amount of GSR incident on a horizontal surface (H), using the equation below [6,11,17,18,20];

$$H = H_o K_r (TR)^{0.5}, \quad (1)$$

where the empirical coefficient $K_r = 0.16$ for 'interior regions' and $K_r = 0.19$ for 'coastal regions' [9,17,20]. The extraterrestrial radiation H_o is given by [6,16,21,22];

$$H_o = \frac{24 \times 3.6 \times 10^{-3} Isc}{\pi} \left[1 + 0.033 cos\left(\frac{2\pi D_n}{365}\right)\right] [cos\phi cos\delta sin\omega_s + \omega_s sin\phi sin\delta], \quad (2)$$

where $Isc = 1367 W/m^2$ is known as the the solar constant [6,16,20], Dn is the Julian calendar day (Jan 1st corresponds to $D_n = 1$, Dec 31st corresponds to $D_n = 365$).
The latitude of the site is denoted by ϕ and all angles are calculated in radians. δ is the declination angle which is given by [6,10,16,21,22];

$$\delta = 23.45 \frac{\pi}{180} sin\left[\frac{2\pi(D_n + 284)}{365}\right]. \quad (3)$$

The sunset hour angle, ω_s is given by [6,20,22,23];

$$\omega_s = cos^{-1}(-tan\phi tan\delta). \quad (4)$$

By calculating the solar angles it is possible to predict the amount of solar irradiance received on a horizontal surface at a given location. The clearness index (K_T) describes the atmosphere's transparency and is found by comparing the amount of GSR to the amount of

extraterrestrial solar radiation as shown by [6,20,21];

$$K_T = \frac{H}{H_o}. \tag{5}$$

The Angstrom-Prescott equation can be used to calculate the clearness index from the relative sunshine duration, provided the Angstrom-Prescott coefficients for the area are known [6,14,15,21];

$$K_T = \frac{H}{H_o} = a + b\left(\frac{S}{S_o}\right), \tag{6}$$

where a, b are the Angstrom-Prescott coefficients, S is the actual hours of sunshine received, and S_o is the maximum possible duration of sunshine for a given day calculated from [15,16,21,23];

$$S_o = \frac{2\omega_s}{15}. \tag{7}$$

For areas where the Angstrom coefficients are unknown, it is prescribed to use $a = 0.25$ and $b = 0.50$ [23].The temperature data of three suburbs in Pietermaritzburg were studied for a full year, namely; Northdale (Residential area), Scottsville (Commercial/ Residential area), and Bisley (Commercial/ Industrial area). A MT668 Temperature and humidity data logger was used to record hourly maximum and minimum temperatures in each location.The Hargreaves-Samani equation was then used to calculate the GSR and compare the results of the three suburbs to determine which area is more suitable for the placement of photovoltaic cells.

Results and Discussion

Daily average measurements of temperature, relative humidity and dew point were recorded

using data loggers calibrated in Northdale, Scottsville and Bisley. Attention to their placement was essential as the sensors, installed at a height of 1,5m above the ground, could not be sheltered (this would alter the recordings drastically) and had to be placed in an open area. Graphs showing the measured maximum and minimum air temperatures (observed during sunrise and sunset) for the three suburbs are illustrated in Figs. 2 and 3.This was conducted for each day of the time period studied (July 2014 - June 2015). The latitude of each suburb was used to calculate the solar angles using eqs. (3) and (4) which then allowed us to calculate the extraterrestrial solar radiation in eq. (2). The Hargreaves-Samani equation (eq.(1)), together with the measured air temperature values gave results which are averaged in Tables; 1,2 and 3.

Table 2: Northdale Results (July 2014- June 2015)

Month	$Tmax$	$Tmin$	H_N	H_{meas}	$RMSE$	$K_{T_N} = \frac{H_N}{H_{ON}}$	$\frac{S}{S_{o_N}}$
Jul	21.89	8.55	11.59	12.41	1.76	0.58	0.66
Aug	24.29	11.43	14.11	13.69	3.20	0.57	0.59
Sep	27.27	12.56	18.96	17.88	4.03	0.61	0.52
Oct	22.83	11.94	19.02	15.34	5.98	0.51	0.47
Nov	23.96	13.84	20.75	14.94	8.01	0.50	0.48
Dec	26.53	15.91	22.09	17.63	6.89	0.51	0.50
Jan	27.98	17.07	22.29	19.69	5.31	0.52	0.46
Feb	26.38	16.44	19.75	19.44	5.67	0.50	0.51
Mar	27.30	16.55	17.73	17.83	3.90	0.52	0.57
Apr	23.98	13.33	13.99	14.58	3.41	0.51	0.66
May	27.62	13.16	13.08	13.76	1.78	0.60	0.75
Jun	22.97	9.52	10.96	12.44	7.06	0.58	0.74
Average	25.25	13.36	17.03	15.80	4.75	0.54	0.58

Table 3: Scottsville Results (July 2014- June 2015)

Month	$Tmax$	$Tmin$	H_S	H_{meas}	$RMSE$	$K_{T_S} = \frac{H_S}{Ho_S}$	$\frac{S}{S_{o_S}}$
Jul	22.16	8.84	11.60	12.41	1.70	0.58	0.66
Aug	24.35	11.46	14.12	13.69	2.99	0.57	0.59
Sep	27.52	12.57	19.08	17.88	4.03	0.61	0.52
Oct	23.06	12.55	18.99	15.34	6.08	0.50	0.47
Nov	24.05	13.92	21.0	14.94	8.30	0.50	0.48
Dec	26.48	15.97	22.10	17.63	6.72	0.51	0.50
Jan	28.20	17.16	22.36	19.69	5.32	0.52	0.46
Feb	26.63	16.63	19.82	19.44	5.80	0.50	0.51
Mar	27.59	16.80	17.72	17.83	4.06	0.52	0.57
Apr	24.17	13.35	14.05	14.58	3.25	0.52	0.66
May	27.72	13.11	13.11	13.76	1.72	0.61	0.75
Jun	21.87	9.78	10.44	12.44	2.97	0.55	0.75
Average	25.32	13.51	17.03	15.80	4.41	0.54	0.58

Table 4: Bisley, Ukulinga Results (July 2014- June 2015)

Month	$Tmax$	$Tmin$	H_B	H_{meas}	$RMSE$	$K_{T_B} = \frac{H_B}{H_{o_B}}$	$\frac{S}{S_{o_B}}$	$K_r(calc)$
Jul	21.83	8.42	11.58	12.41	1.76	0.58	0.66	0.182
Aug	23.37	11.24	14.01	13.69	3.04	0.56	0.59	0.202
Sep	27.18	12.36	19.00	17.88	3.94	0.61	0.52	0.198
Oct	22.67	12.36	18.83	15.34	5.89	0.50	0.47	0.190
Nov	23.43	13.92	20.30	14.94	7.68	0.48	0.48	0.183
Dec	26.04	15.96	21.66	17.63	6.48	0.50	0.50	0.193
Jan	27.76	17.10	22.00	19.69	5.90	0.51	0.46	0.181
Feb	26.23	16.55	19.50	19.44	5.63	0.49	0.51	0.175
Mar	27.08	16.76	17.33	17.83	4.01	0.51	0.57	0.173
Apr	23.86	13.51	13.65	14.58	3.40	0.50	0.66	0.179
May	25.81	12.81	12.33	13.76	2.22	0.57	0.75	0.174
Jun	21.97	9.66	10.66	12.44	2.84	0.57	0.75	0.166
Average	24.77	13.39	16.74	15.80	4.40	0.53	0.58	0.183

The data supplied by the ARC allowed us to compare the values calculated by eq. (1) with the actual measured data. These measured values are listed in Tables: 2-4 as $H_{measured}$. The Hargreaves Samani empirical coefficient K_r was determined from the measured Bisley temperature data (Table 4) , but showed high inconsistency making it not suitable for use in the model. This could be a result of the influence of other meteorological factors (topography, cloudiness, relative humidity, wind speed, advection) on the air temperature. Temperature variations for all three cities show a similar distribution to the H (both observed and calculated) values which illustrates the relationship between air temperature and GSR . The daily Root Mean Square Errors were calculated using;$RMSE = \sqrt{\frac{\sum_{i=1}^{n}(\hat{y}_i - y_i)^2}{n}}$, where $\hat{y}_i$ is the calculated values of H (H_N, H_S, H_B), and y_i is $H_{measured}$. The annual average $\overline{RMSE} = 4.52 MJ/m^2$ indicates the standard deviation of the calculated values of H from the observed values. This shows a large deviation in the data predicted using the model when compared to the data observed. This error mainly arises from the RMSE in the summer months. The calculated values of H in each suburb of Pietermaritzburg conformed well to the shape of the data observed by the ARC, with the exception of a few outliers. This is represented in Figs.; 4,5,6 and 7. Maximum calculated values for H were observed during October - January (Fig. 7) which are the Spring and Summer months in South Africa. The Hargreaves-Samani model produced the most deviation from the measured GSR values in these Spring/ Summer months which is visible in Fig. 7.

The model over predicted values of GSR and errors could be a consequence of; the accuracy and efficiency of the equipment used, placement of the equipment, the effects of wind, or other temperature invasion factors. Observed values could be better validated by adjusting this temperature based model to account for short wave radiation and other meteorological factors such as relative humidity which may have endorsed these errors. During the Autumn, Winter and parts of Spring months, the model performed considerably well in estimating the amount of GSR This is shown in Fig. 7. Overall, the distribution and monthly variation of the calculated values of GSR show great similarities when compared to the observed values

(See Figs : 4-6).

The annual average GSR values obtained for Pietermaritzburg, show close similarities to the results presented by Maluta et al. [20], for the Limpopo Province in South Africa. In the study conducted by [20], stations which have an altitude close to that of Pietermaritzburg, had an annual average H value in the range; $[14.71 - 17.82]\ MJ/m^2$, whilst H_{calc} for Pietermaritzburg is in the range; $[16.79 - 17.00]\ MJ/m^2$. The main contributing difference in these locations is the site's latitude.

The clearness index, being the ratio of GSR to extraterrestrial radiation provides information on the degree of transparency of the atmosphere. Using eq. (5); K_{T_N}, K_{T_S}, K_{T_B}were calculated and interpreted by the following work conducted in [6];

Table 5:Classification of Day by Clearness Index

Day Type	K_T
Clear	$0.7 \leq K_T < 0.9$
Partially cloudy	$0.3 \leq K_T < 0.7$
Cloudy	$0.0 \leq K_T < 0.3$

Our results showed a high number of partially cloudy days, with not many days being classified as cloudy using Table 5. The errors experienced in the calculated $H$and $H_o$values may be a result of the influence of cloudiness on the air temperature data. On average, the monthly data gives a clearness index which falls into the partially cloudy category for all three suburbs in question (Tables 2-4). The maximum possible sunshine duration eq. (7) was calculated using the hour angle eq. (4). Data of the available sunshine hours in Pietermaritzburg was used to then find the relative sunshine duration for each month. In Figs.; 8-10, a linear fit was used to correlate values of K_T with values of $\frac{S}{S_o}$ in order to determine the Angstrom coefficients a, b using the Angstrom-Prescott equation in eq. (6). The regression line is

labeled as f(x). The coefficient a is the intercept of the axis which represents K_T while, the b -coefficient is found from the gradient of the regression line. Results are graphically represented in Figs.; 8,9 and 10. Using the linear fit, the following Angstrom coefficients were found;

Table 6: Angstrom Coefficients (July 2014- June 2015)

Town	a-coefficient	b-coefficient	r
Northdale	0.26 ± 0.01	0.39 ± 0.06	0.629
Scottsville	0.23 ± 0.10	0.41 ± 0.06	0.567
Bisley	0.24 ± 0.11	0.40 ± 0.07	0.554
Average	0.24 ± 0.07	0.40 ± 0.06	0.583

The results presented in Table 6 compare fairly well to the prescribed values for a, and b which are given by [23] as; $a = 0.25$, $b = 0.50$ for a location where these coefficients are not known. The Angstrom coefficients vary with each geographical location depending on the amount of relative sunshine received. The large deviation of the Angstrom b coefficient is a result of errors encountered in the fraction of sunshine duration. Since temperature measurements were taken on mostly partially cloudy days, the calculated GSR values were not entirely accurate and hence the maximum possible sunshine duration measurements S_o are inaccurate. Other factors such as the geographical locations of the sites and atmospheric effects may also introduce deviations from the suggested Angstrom coefficients. For a more reliable set of Angstrom coefficients, this study should be extended to analyze data over a longer period of time for the chosen location. Results obtained for the period July 2014- June 2015, lead to the assumption that the Angstrom-Prescott equation for Pietermaritzburg is; $\frac{H}{H_o} = 0.247 + 0.460\frac{S}{S_o}$. On calculation of the Pearson correlation coefficient $r = \frac{n\sum xy - (\sum x)(\sum y)}{\sqrt{[n\sum x^2 - \left(\sum x\right)^2].[n\sum y^2 - \left(\sum y\right)^2}}$, for each regression model, an average value of $r = 0.583$ was obtained. This illustrates a moderate/weak linear relationship between the clearness index K_T and the relative sunshine duration $\frac{S}{S_o}$ in Pietermaritzburg. This poor relationship can be explained by the influences of other meteorological factors (rainfall, wind speed,

cloudiness, humidity) on the measured temperatures and calculated data sets. To realise a stronger correlation and set of Angstrom coefficients, the equipment needs to be modified to obtain more accurate readings and the HS model needs to be adjusted to account for the influences of various climatic factors.

The results obtained in this study indicate that the city of Pietermairtzburg receives sufficient GSR for the use of solar powered technologies such as solar panels, solar heating and cooling technologies for Industrial, Commercial and Residential areas. Accurate GSR predictions for this city will also enable a better understanding of the climate experienced and its effects. Clear days are experienced throughout the year, including during the Winter months, making GSR easy to acquire. The Hargreaves Samani model is suitable for the calculation of GSR, however the accuracy of results during the summer season is not reliable. Adjustments need to be made to the model to account for this.

Measurement of the Angstrom Prescott coefficients allows us a second simple method to verify the ratio of GSR to extraterrestrial radiation received at a location. These coefficients give insight into the transmissivity and transparency of the atmosphere. Prediction of the type of day and clearness index can also be made, provided the Angstrom coefficients are well-established. Though solar radiation data in the city of Pietermaritzburg is not readily available, the amount of GSR incident in this city can be sufficiently estimated using the Hargreaves-Samani model. This study has shown the suitability of this interior region to contribute to the decrease in demand of grid energy by making use of the incident GSR in Pietermaritzburg.

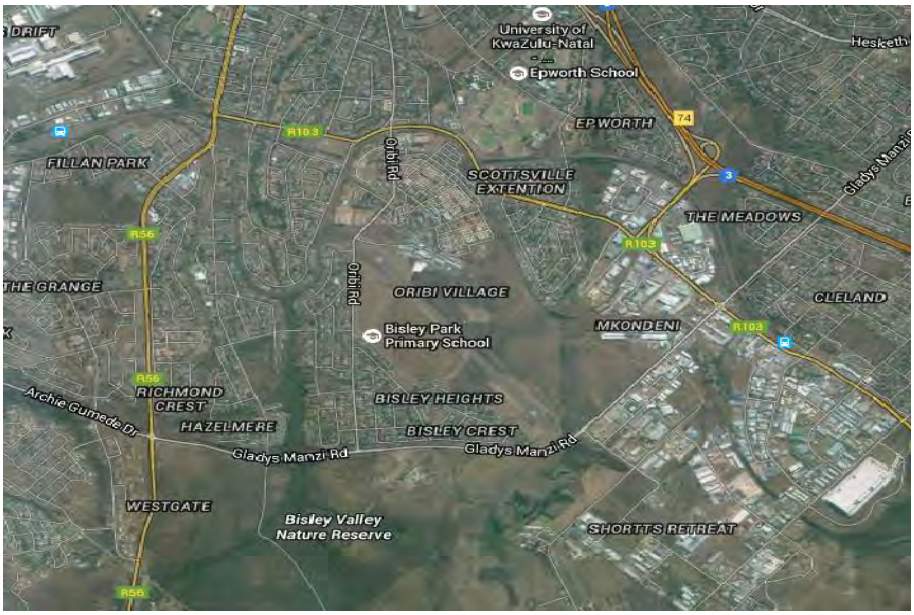

Figure 1: Satellite image of Scottsville, Bisley [google maps].

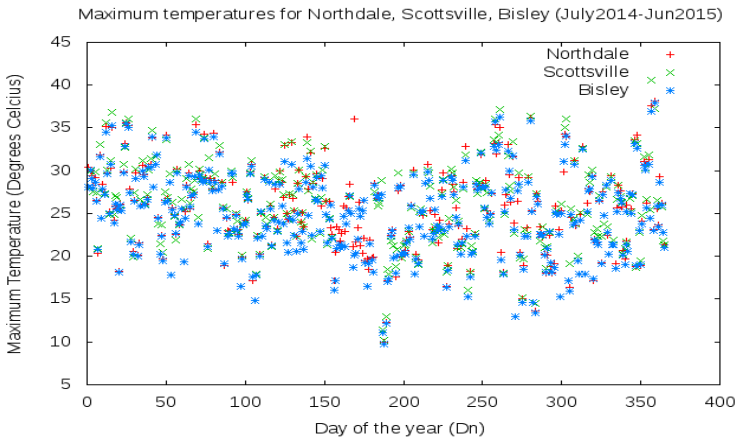

Figure 2: Graph of measured Maximum temperatures.

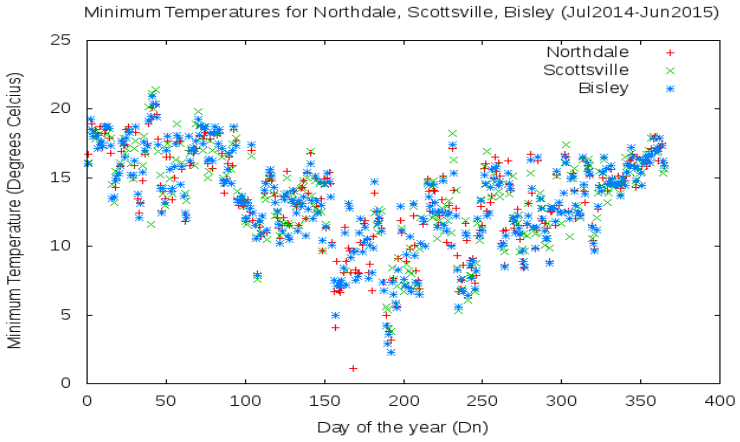

Figure 3: Graph of measured Minimum temperatures.

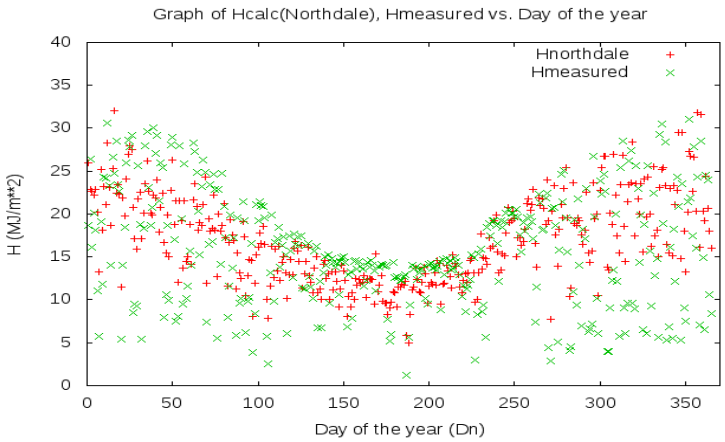

Figure 4: Graph of Hcalculated vs. Hmeasured in Northdale.

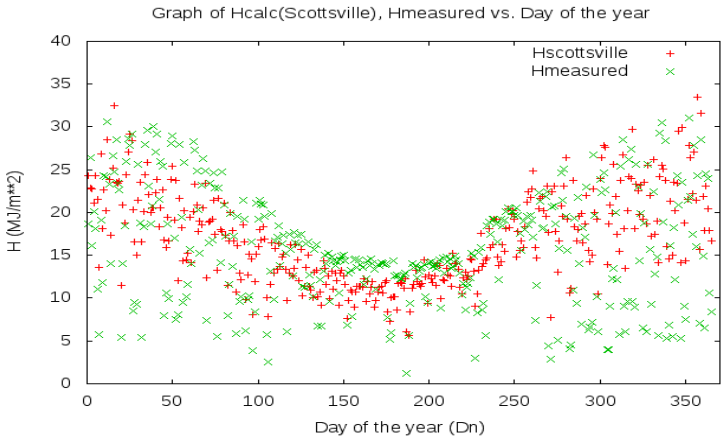

Figure 5: Graph of Hcalculated vs. Hmeasured in Scottsville.

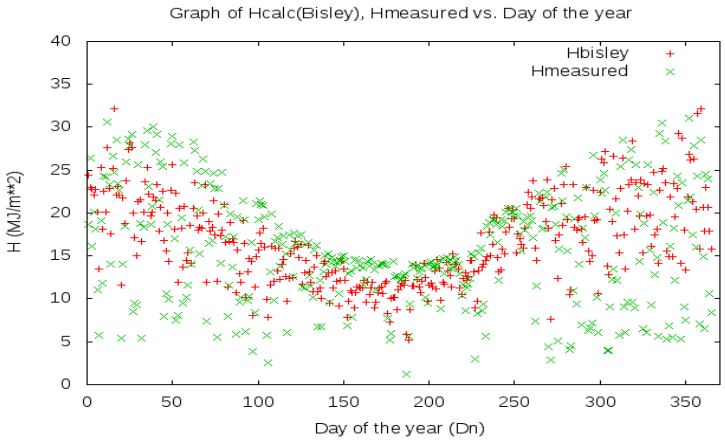

Figure 6: Graph of Hcalculated vs. Hmeasured in Bisley.

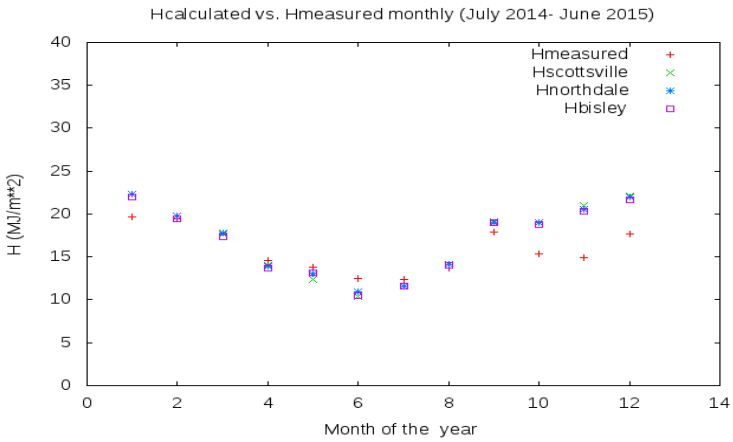

Figure 7: Graph of monthly Hcalculated values vs. Hmeasured.

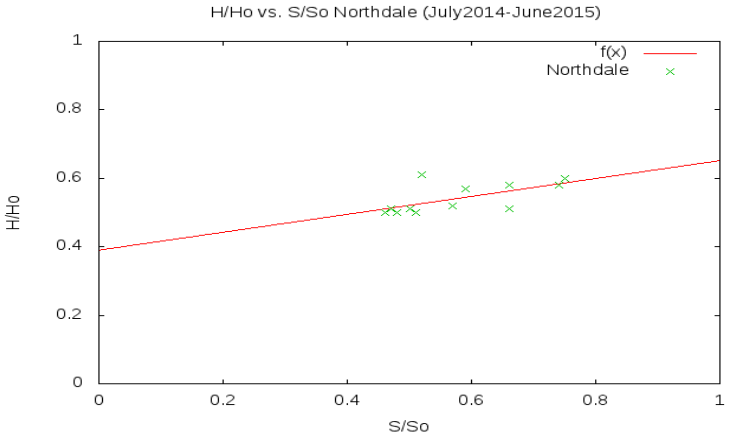

Figure 8: Graph of H/Ho vs. S/So to determine Angstrom coefficients for Northdale.

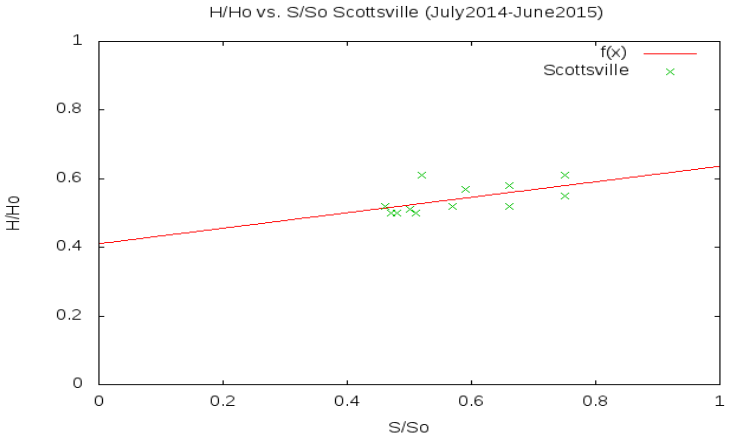

Figure 9: Graph of H/Ho vs. S/So to determine Angstrom coefficients for Scottsville.

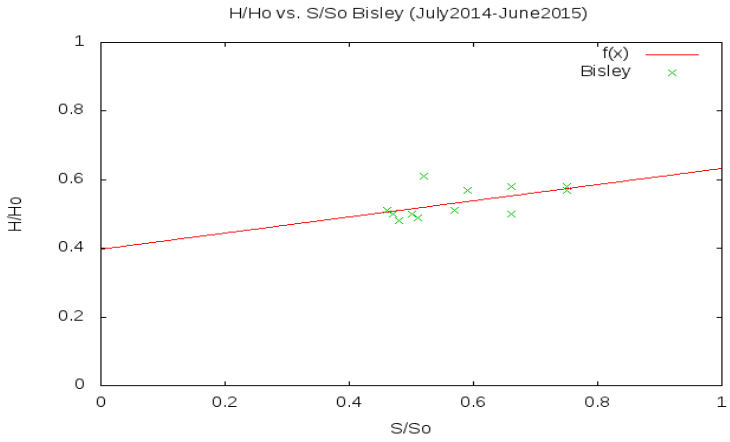

Figure 10: Graph of H/Ho vs. S/So to determine Angstrom coefficients for Bisley.

Conclusions

The use of the Hargreaves-Samani equation proves to be an adequate model to estimate the amount of GSR in locations where solar radiation data is not readily available. Our results show that this model has compared considerably well to the measured values of GSR for the city of Pietermaritzburg. However, the accuracy of this model can be improved by adjusting the equation to account for; more than one meteorological parameter (sunshine duration, relative humidity), shorter forecasting horizons and the inclusion of short wave radiation [23].

The results herein, show the degree of simplicity such a model has, based on the use of one weather parameter alone. The Hargreaves-Samani equation is viable for use in any geographical location since its dependency is mainly on the location and air temperature of a given site. Establishing a reliable set of Angstrom-Prescott coefficients will allow us to make use of available sunshine duration data in order to predict the clearness index and hence the ratio of global to extraterrestrial solar radiation. For this to be accomplished, it is suggested that we analyze the data for this city over a longer period ($\pm$10 calendar years prior to current data). However, the results we have obtained in just one calendar year show close proximity to the prescribed values of the Angstrom coefficients for locations where this

information is unknown. The weak correlation between the sunshine duration and clearness index indicates discrepancies experienced in the results. This may be a result of various meteorological factors which have influenced the air temperature measurements as well as the GSR calculations. KwaZulu-Natal is said to be unsuitable for the construction of large scale solar power plantations, primarily due to the low amount of Direct Normal Irradiation (DNI) incident in this province as opposed to the other eight provinces in South Africa [24]. Despite this, our province still receives ample sunshine duration and GSR for the utilization of solar technologies such as photovoltaic cells (both in Industry and for household consumption).

Acknowledgements

The authors would like to acknowledge the assistance of Mr. Richard Kunz of the University of KwaZulu-Natal Research center in Ukulinga, Bisley; The ARC (Cedara) who provided data to the Ukulinga Research Farm. The financial assistance of the National Research Foundation (DAAD-NRF) towards this research is hereby acknowledged. Opinions expressed and conclusions arrived at, are those of the author and are not necessarily to be attributed to the DAAD-NRF.

References

[1] Govinda R.T., Lado K., Patrick A. N. A review of solar energy, markets, economics and policies. Policy research working paper. The world bank, development and research group, environment and energy team. October 2011. Available from : http://econ.worldbank.org

[2] Eskom web page [Internet]. http://www.eskom.co.za/AboutElectricity/ElectricityTechnologies/Pages/Coal_Power.aspx

[3] Renewable Energy| Department: Energy| Republic of South Africa [Internet]. http://www.energy.co.za/files/esources/renewables/r_solar.html

[4] Qiang Fu. Radiation (Solar). University of Washington, Seattle, WA, USA. Elsevier Ltd. 2003

[5] Sayigh A. A. M. Solar radiation availability prediction from climatological data. Academic Press, New York. 1977. pp.61. ISBN: 0-12-620850-6

[6] Viorel B. Modeling solar radiation at the earth's surface: Recent advances. Springer. 2008. ISBN: 3540774548

[7] Boeker E., Van Grondelle R. Environmental physics: Sustainable energy and climate change. 3rd Edition. John Wiley and Sons Ltd. 2011

[8] Kennewell J., McDonald A. IPS-Satellite communications and space weather [Internet]. The Australian Space Weather Agency. 2008. Available from: http://www.ips.gov.au/Educational/1/3/2

[9] Almorox J., Hontoria C., Benito M. Models for obtaining daily global solar radiation with measured air temperature data in Madrid (Spain). Applied Energy 88. 2011. pp. 1703-1709. DOI: 10.1016/japenergy.2011.11.003

[10] Tijjani B.I. Comparison between first and second order Angstrom type models for sunshine hours in Katsina Nigeria. Bayero Journal of Pure and Applied sciences. Vol 4(2). pp. 24-27. Available from: dx.doi.org/10.4314/bajopas.v4i2.5

[11] Rahimikoob A. Estimating global solar radiation using ANN and air temperature data in semi-arid environment (Iran). Renewable Energy. Vol. 35. 2010. pp.2131-2135. DOI:10.1016/j.renene.2010.01.029

[12] Al Riza D. F., Gilani S. I., Aris M. S. Hourly solar radiation estimation using ambient temperature and relative humidity data. International Journal of Environmental Science and Development. Vol. 2(3). June 2011.

[13] Gadiwala M. S. Usman A., Akhtar M., Jamil K. Empirical models for the estimation of global solar radiation with sunshine hours on horizontal surface in various cities of Pakistan. Pakistan Journal of Meteorology. Vol. 9(18). Jan 2013

[14] Angstrom A. Solar and atmospheric radiation. International commission for solar research on Actinometric Investigations of solar and atmospheric radiation. Journal of the Royal Meteorological Society. pp.121-126. 1923

[15] Srivasta R. C., Pandey H. Estimating Angstrom-Prescott coefficients for India and developing a correlation between sunshine hours and global solar radiation for India. ISRN Renewable Energy. Vol 2013. Hindawi Publishing. Available form: http://dx.doi.org/10.1155/2013/403742

[16] Ituen Eno E., Esen Nisken U., Nwokolo Samuel C., Uto Ema G. Prediction of Global solar radiation using relative humidity, maximum temperature and sunshine hours in Uyo in the Niger delta Region, Nigeria. Advances in Applied Science Research. Vol. 3(4). pp.1923-1937. 2012. ISSN: 0976-8610

[17] Samani Z. Estimating solar radiation and evapotranspiration using minimum climatological data. Journal of Irrigation and Drainage Engineering. July 2000. pp. 265-267.

[18] Allen R.G. Self-calibrating method for estimating global solar radiation from air temperature. Journal of Hydrologic Engineering. New York. Vol.2. 1991. pp. 56-57. ISSN: 10840699

[19] Hargreaves G. H., Samani Z. A. Estimating potential evapotranspiration. Journal of irrigation and drainage engineering. ASCE. 108(IR3). 1982. pp.223-230

[20] Maluta E. N., Maludzi T. S., Sankaran V. Estimation of the global solar radiation on the horizontal surface from temperature data for the Vhembe district in the Limpopo province of South Africa. International journal of green energy. Vol. 11(5). Nov 2013. pp. 454-464. DOI: 10.1080/15435075.2013.772518

[21] Salima G., Chavula G.M.S. 'Determining Angstrom coefficients for estimating solar radiation in Malawi'. International Journal of Geosciences, (3), pp.391-397. (2012)

[22] Teke A., Yildirim H.B. 'Estimating the monthly global solar radiation for Eastern Mediterranean Region'. Energy conversion and Management 87, pp.628-635. (2014)

[23] Allen R.G., Pereira S.L., Raes D., Smith M. 'FAO Irrigation and Drainage paper No.56. Crop evapotranspiration (Guidelines for computing crop water requirements). 1977

[24] Fluri T.P. 'The potential of concentrating solar power in South Africa'. Energy Policy 37(2009). pp.5075-5080

APPENDIX A

FORTRAN CODE TO CALCULATE GSR

```
program solarcalculation
!This program allows the user to calculate the GSR for a given site of latitude phi, by using daily maximum and minimum temperatures, for the Julian day (Dn)

implicit none

real:: delta, d, omega
! Declares required variables

real:: phi, Isc, Ho
real:: H, Kr, Tmax
real:: Tmin, TR, pi
real:: E, X, s, Kt!
real:: y, z, theta, So

! Declaring variables s, y, z which are dummy variables

print*, "Enter the Julian day Dn"
! Prompts user to input Dn
read*, d
! Stores Dn as d

print*, “Enter the value of phi (latitude of site)”
! Prompts user to input phi
read*, phi
! Stores phi

print*, "Enter maximum temperature for the day"
! Prompts user to input Tmax
```

```
read*, Tmax
! Stores Tmax

print*, "Enter minimum temperature for the day"
! Prompts user to input Tmin
read*, Tmin
! Stores Tmin

Isc= 1367.0
! Initializes solar constant Isc
pi= 4.0*ATAN(1.0)
! pi = 3.1415
Kr= 0.162
! Initializes empirical coefficient for H-S equation
TR= Tmax-Tmin
! Defines temperature range TR

y= (360.0*(284+d))/365.0

delta= ((23.45*pi/180.0)*SIN((y*pi)/180.0))
! Calculates delta in radians

E= ((24.0*3.6e-3*Isc)/pi)
! Calculates eccentricity coefficient

s=(phi*pi)/180.0
! Converts phi to radians

omega = ACOS(-1*(TAN(s))*(TAN(delta)))
! Calculates omega in radians

z= 360.0*(d/365.0)
```

```
X= (1+(0.033*(COS((z*pi)/180.0))))
! Calculates the Sun-Earth distance

Ho= (E * X *(COS(s)*COS(delta)*SIN(omega) + omega*SIN(s)*SIN(delta)))
! Calculates ETR

H= (Kr*Ho) * (sqrt(TR))
! Calculates GSR according to H-S equation
So= ((2.0/15.0)*(omega*180.0/pi))
! Calculates maximum sunshine hours
Kt= H/Ho
! Calculates clearness index

Print*, "delta is",delta, “radians”
Print*, "omega is",omega, “radians”
Print*, "Ho is",Ho, “MJ/m^2”
Print*, "H is ",H, “MJ/m^2”
print*, "So is ,",So, “hours”
Print*, "Kt, clearness index is” ,Kt
! Outputs calculated values of delta, omega, Ho, H, So and Kt

End program solarcalculation
```

APPENDIX B

DAILY RESULT REPORT (JULY 2014 - JUNE 2015)